Report No. CDOT-DTD-R-2004-03
Final Report

LONG-TERM DURABILITY OF FIBER-REINFORCED POLYMERS (FRPS) AND IN-SITU MONITORING OF FRP BRIDGE DECKS AT O'FALLON PARK BRIDGE

Yunping Xi
Sunyoung Chang
Andi Asiz
Yue Li

DEPARTMENT OF TRANSPORTATION
RESEARCH

April 2004

COLORADO DEPARTMENT OF TRANSPORTATION
RESEARCH BRANCH

The contents of this report reflect the views of the authors, who (are) responsible for the facts and accuracy of the data presented herein. The contents do not necessarily reflect the official views of the Colorado Department of Transportation or the Federal Highway Administration. This report does not constitute a standard, specification, or regulation.

Technical Report Documentation Page

1. Report No. CDOT-DTD-R-2004-03	2. Government Accession No.	3. Recipient's Catalog No.
4. Title and Subtitle LONG-TERM DURABILITY OF FIBER-REINFORCED POLYMERS (FRPS) AND IN-SITU MONITORING OF FRP BRIDGE DECKS IN O'FALLON PARK BRIDGE		5. Report Date April 2004
		6. Performing Organization Code
7. Author(s) Yunping Xi, Sunyoung Chang, Andi Asiz, Yue Li		8. Performing Organization Report No. CDOT-DTD-R-2004-03
9. Performing Organization Name and Address Department of Civil, Environmental, and Architectual Engineering University of Colorado at Boulder Engineering Center ECOT 441, UCB 429, Boulder, CO 80309		10. Work Unit No. (TRAIS)
		11. Contract or Grant No. 87.30
12. Sponsoring Agency Name and Address Colorado Department of Transportation - Research 4201 E. Arkansas Ave. Denver, CO 80222		13. Type of Report and Period Covered
		14. Sponsoring Agency Code

15. Supplementary Notes

16. Abstract

Glass fiber reinforced polymers (GFRPs) were selected and used to build the bridge deck for O'Fallon Park Bridge in Denver, Colorado. This report contains two parts. The first part is an in-house experimental study on the durability of the selected GFRPs, and the second part is an on-site loading test for the behavior of one GFRP panel of the bridge and a long-term monitoring study of the panel. The influential parameters for the durability of GFRPs were reviewed, including freeze-thaw cycles, moisture penetration, deicing chemicals, alkali and acid attacks, and ultraviolet light. Experimental plans were carefully designed for the in-house durability study and the on-site loading test, as well as for the long-term monitoring of the bridge panel.

Every environmental parameter tested in the study resulted in a degradation of GFRPs to a certain extent. From the strength aspect, the worst degradation was a 35% reduction of tensile strength of the GFRP subjected to the ponding of 1M NaOH solution. From the stiffness point of view, the worst degradation was a 32% reduction of Young's modulus of the GFRP subjected to the ponding of 3% $Ca(Cl_2)$ solution.

The strains due to the mechanical loading (a CDOT truck) are very small. Therefore, the structural design of the GFRP panel for O'Fallon Park Bridge is very conservative. Comparing the effect of environmental temperature with the effect of mechanical loading, it is very clearly that the effect of temperature is dominant. Therefore, in addition to the mechanical fatigue loading test performed in this project, a larger scale cyclic temperature test for the FRP panel is very necessary and important for evaluating the long-term performance of the panel.

Implementation:
The significant degradations in terms of the tensile strength and the stiffness must be considered in the specifications related to the structural design of bridge decks if the GFRP is to be used widely for bridge decks in the state of Colorado. The monitoring process of the bridge deck should be continued. The results obtained so far provide valuable information and can be compared to the strains that will be collected in the future to evaluate the long-term performance of the bridge deck.

17. Keywords GFRPs, environemental conditions, fatigue loading, freeze-thaw, moisture penetration, deicers	18. Distribution Statement No restrictions. This document is available to the public through the National Technical Information Service 5825 Port Royal Road Springfield, VA 22161

19. Security Classif. (of this report)	20. Security Classif. (of this page)	21. No. of Pages	22. Price
None	None	59	

Form DOT F 1700.7 (8-72) Reproduction of completed page authorize

LONG-TERM DURABILITY OF FIBER-REINFORCED POLYMERS (FRPS) AND IN-SITU MONITORING OF FRP BRIDGE DECKS AT O'FALLON PARK BRIDGE

by

Yunping Xi, Sunyoung Chang, Andi Asiz, and Yue Li

Report No. CDOT-DTD-R-2004-03
Final Report

Prepared by
University of Colorado at Boulder

April 2004

The Colorado Department of Transportation
Research Branch
4201 E. Arkansas Ave.
Denver, CO 80222
(303) 757-9506

Acknowledgements

The financial support provided by the Colorado Department of Transportation for this study is gratefully acknowledged. Partial financial support under NSF grant ACI-0112930 to University of Colorado at Boulder is gratefully acknowledged.

The GFRP bars for the test were provided free of charge by Kansas Structural Composites, Inc. of Russell, USA.

The writers would like to express their thanks to the Colorado DOT for continuous support and encouragement throughout this study, and specifically to Ahmad Ardani and Richard Griffin of CDOT Research Branch; Trever Wang, Ali Haraj, and Michael McMullen of CDOT Staff Bridge; Greg Lowery of CDOT Staff Materials; and Matt Greer of FHWA for their valuable suggestions and input.

EXECUTIVE SUMMARY

Fiber-reinforced polymers (FRPs) are increasingly being used as reinforcement in new concrete structures and as strengthening materials for the rehabilitation of existing concrete structures. Among various types of FRP materials, glass fiber reinforced polymers (GFRPs) were selected and used to build the bridge deck for O'Fallon Park Bridge in Denver, Colorado. Although much research has been done on the mechanical properties of FRPs, the overall long-term durability of GFRPs under severe environmental conditions has not been systematically evaluated. This is the major focus of the present report, which contains two parts. The first part is an in-house experimental study on the durability of the selected GFRPs, and the second part is an on-site loading test for the behavior of one GFRP panel of the bridge and a long-term monitoring study of the panel.

The influential parameters for the durability of GFRPs were reviewed, including freeze-thaw cycles, moisture penetration, deicing chemicals, alkali and acid attacks, and ultraviolet light. Experimental plans were carefully designed for the in-house durability study and the on-site loading test, as well as for the long-term monitoring of the bridge panel.

Every environmental parameter tested in the study resulted in a degradation of GFRPs to a certain extent. From the strength aspect, the worst degradation was a 35% reduction of tensile strength of the GFRP subjected to the ponding of 1M NaOH solution. From the stiffness point of view, the worst degradation was a 32% reduction of Young's modulus of the GFRP subjected to the ponding of 3% $Ca(Cl_2)$ solution.

For future work, it is suggested that the degradation of FRP should be tested with coupling effects. Due to coupling effects between moisture and elevated temperatures, the degradation could be accelerated by high diffusion rates. Additionally, the freeze-thaw, alkali attack, UV radiation, and moisture can be applied concurrently to see how the combinations of the influential parameters affect the degradation of the FRP specimens. For the ponding test, the

weights of specimens before and after ponding should be measured and compared. This is an important factor for measuring the moisture intake capacity of the GFRP specimens.

The strains due to the mechanical loading (a CDOT truck) are very small. Therefore, the structural design of the GFRP panel for O'Fallon Park Bridge is very conservative.

Comparing the effect of environmental temperature with the effect of mechanical loading, it is very clear that the effect of temperature is dominant. The maximum strain due to the mechanical loading is 226 microstrain, while the thermal strains in the winter are all higher than that. This means that the temperature variation is more important than the variation of mechanical loading. Therefore, in addition to the mechanical fatigue loading test performed in this project, a larger scale cyclic temperature test for the FRP panel is very necessary and important for evaluating the long-term performance of the panel.

IMPLEMENTATION STATEMENT

The significant degradations in terms of the tensile strength and the stiffness must be considered in the specifications related to the structural design of bridge decks if the GFRP is to be used widely for bridge decks in the state of Colorado.

The monitoring process of the bridge deck should be continued. The results obtained so far provide valuable information and can be compared to the strains that will be collected in the future to evaluate the long-term performance of the bridge deck.

TABLE OF CONTENTS

1. Long-Term Durability of Glass FRPs....8
1.1 Introduction.... 8
1.2 Influential Parameters for the Durability of FRPs.... 8
1.3 Experimental Plan.... 11
1.3.1 Specimen preparation.... 11
1.3.2 Conditioning of specimens.... 12
1.3.3 Uniaxial tension tests.... 17
1.4 Experimental Results.... 17
1.5 Suggestions for Future Reseach.... 25
2. In-situ Monitoring of the GFRP Deck Panel....26
2.1 Introduction.... 26
2.2 Installation of Fiber Optic Sensors.... 27
2.3 In-situ Monitoring of the Bridge Decks.... 31
2.3.1 Results of truck loading test.... 31
2.3.2 Temperature effect.... 37
3. Conclusions and Recommendations....41
3.1 Durability of GFRPs.... 41
3.2 Monitoring of the Bridge Deck.... 42
4. References....44

Appendix A. Uniaxial Tension Test Data for Durability of GFRP Specimens....47
A.1 Conditioning: Room temperature (Unexposed).... 47
A.2 Conditioning: Freeze-Thaw Cycles.... 48
A.3 Conditioning: Wetting-Drying Cycles in Water.... 48
A.4 Conditioning: $Mg(Cl_2)$ 3% Ponding Test.... 49
A.5 Conditioning: $Ca(Cl_2)$ 3% Ponding Test.... 49
A.6 Conditioning: NaCl 3% Ponding Test.... 50
A.7 Conditioning: $Mg(Cl_2)$ 3% Cyclic Test.... 50
A.8 Conditioning: $Ca(Cl_2)$ 3% Cyclic Test.... 51
A.9 Conditioning: NaCl 3% Cyclic Test.... 51
A.10 Conditioning: 1M NaOH Ponding Test.... 52
A.11 Conditioning: 1M HCl Ponding Test.... 52
A.12 Conditioning: Ultraviolet Radiation Test.... 53

Appendix B. Strain History of O'Fallon Park Bridge due to Temperature Effect..54

LIST OF FIGURES

Figure 1. The environment chamber used in the project 12
Figure 2. Freeze-thaw cycling program for a 12-hour period.. 13
Figure 3. The wetting and drying apparatus 14
Figure 4. Immersion of FRP specimens in three solutions of deicing chemicals 15
Figure 5. Ultraviolet Radiation Apparatus... 16
Figure 6. Experimental setup for uniaxial tension test of a GFRP specimen 16
Figure 7. The failure mode of a GFRP Specimen... 18
Figure 8. Tensile stress-strain curves of a GFRP bar after the freeze-thaw cyclic testing............ 18
Figure 9. A tensile stress-strain curve of a GFRP specimen after wetting/drying cycles in water20
Figure 10. Comparison of mechanical properties of GFRP specimens exposed to deicing chemicals (the ponding test) (a) Ultimate tensile strength; and (b) Young's modulus 21
Figure 11. Comparison of mechanical properties of a GFRP bar exposed to deicing chemicals (Ponding test) (a) Ultimate tensile strength; and (b) Young's modulus 23
Figure 12. Fiber-Reinforced Polymer Honeycomb (FRPH) Sandwich Panels............................. 26
Figure 13. The bridge in O'Fallon Park, Denver, Colorado 27
Figure 14. Fiber optic strain gage 28
Figure 15. Installation of fiber optic sensors in the FRPH panel.. 28
Figure 16. The locations of fiber optic sensors in the FRPH panel 29
Figure 17. Installation of the fiber optic strain gage monitoring system 30
Figure 18. Load test for the bridge (a CDOT dump truck)... 31
Figure 19. The axle load of the CDOT truck 32
Figure 20. The location of the rear axle in the loading test 1 33
Figure 21. Microstrain distributions in Section A-A 33
Figure 22. The location of the rear axle in the loading test 2 34
Figure 23. Microstrain distributions in Section B-B... 34
Figure 24. The location of the rear axle in the loading test 3 35
Figure 25. Microstrain distributions in Section A-A 35
Figure 26. The location of the rear axle in the loading test 4 36
Figure 27. The microstrain distribution in Section B-B 36
Figure 28. Temperature profiles at the top and bottom surfaces of the panel 37
Figure 29. Longitudinal microstrains versus time in the top of the panel 38
Figure 30. Longitudinal microstrains versus time in the bottom of the panel 39
Figure 31. Transverse microstrains versus time in the panel due to the temperature effect......... 40

LIST OF TABLES

Table 1. Mechanical properties of GFRP specimens after the freeze-thaw cyclic testing 19
Table 2. Mechanical properties of GFRP specimens after wetting/drying cycles in water.......... 19
Table 3. Mechanical properties of GFRP specimens exposed to deicing chemicals.................... 20
Table 4. Mechanical properties of a GFRP bar exposed to decing chemicals.............................. 22
Table 5. Mechanical properties of GFRP specimens exposed to alkaline attack 24
Table 6. Mechanical properties of GFRP bar exposed to ultraviolet radiation 24

1. Long-Term Durability of Glass FRPs

1.1 Introduction

Fiber-reinforced polymers (FRPs) are increasingly being used as reinforcement in new concrete structures and as strengthening materials for the rehabilitation of existing concrete structures. The main advantages of FRPs are their light weight, high strength, and non-corrosive features. Among several types of FRP materials available, glass fiber reinforced polymers (GFRPs) were selected and used to build the bridge deck for O'Fallon Park Bridge in Denver, Colorado. The details on the bridge design and structural analysis of bridge decks can be found elsewhere. (Camat and Shing 2004).

Much research has been done on the mechanical properties of FRPs, and FRP bridge decks have been used in several states in the United States. However, the overall long-term durability of the materials under severe environmental conditions has not been systematically evaluated. This is the major focus of the present report. In order to assess the durability behavior of FRPs in a reasonable period of time, various accelerated aging tests were employed in this study to investigate the deterioration of mechanical properties of GFRP plates in service environments.

1.2 Influential Parameters for the Durability of FRPs

Freeze-thaw cycles

The FRP materials are subjected to freeze-thaw cycles in cold region environments. The influence of freeze-thaw cycles may change the material properties of the FRP. Microcracks and voids in the polymer matrix can occur in FRP materials during a freeze-thaw cycling due to the mismatch of the coefficients of thermal expansion (CTE) of fibers and resin. Because of CTE mismatch and the appearance of the cracks, thermal fatigue can be induced between the fibers and matrix.(Tannous and Saadatmanesh 1998) Dutta (Dutta 1988) reported that the FRPs subjected to 150 cycles between -40 °C and +23.4 °C exhibited a 10% reduction in the tensile strength. Gangarao and Vijay (Gangarao and Vijay 1997) reported that GFRPs with seven resin types exhibited a 6% loss in tensile strength when exposed to freeze-thaw cycles in a period of 141 days. The same GFRPs when exposed to alkali conditioning showed a 49% loss in tensile strength.

Moisture penetration

Moisture diffusion into an epoxy matrix and the susceptibility of the glass fibers to water causes changes in thermophysical, mechanical and chemical characteristics of FRPs. (Jones 1999; Shen et al., 1976) Moisture in the resin weakens the Van der Walls force between the polymer chains, and results in a significant degradation of the FRP material's Young's modulus, strength, and glass transition temperature. The swelling stress induced by the moisture uptake can also cause matrix cracking and fiber-matrix debonding (Hayes et al., 1998). GFRPs are particularly sensitive to the influence of moisture content. Hayes et al.(Hayes et al., 1998) reported that the tensile strength and Young's modulus of glass/vinyl ester laminate was reduced by 26% due to wetting/drying cycles at 45^{o}C after 30 days. Bank et al. (Bank et al., 1998) conducted moisture exposure tests on E-glass/vinyl ester rods that were immersed in water at 40^{o}C and 80^{o}C. The flexural strength of the material was reduced by 85% and 55% at 40^{o}C and 80^{o}C, respectively. Porter and Barnes (Porter and Barnes 1998) exposed a FRP specimen to air at 100% RH at temperatures of 93^{o}C and 23^{o}C for 200 days. Reductions in the tensile strength of the E-glass/vinyl ester laminate were 40% and 25% at 93^{o}C and 23^{o}C, respectively. Verghese et al. (Verghese et al., 1998) studied the effects of moisture uptake and temperature on mechanical properties of FRP materials.

The coupling effect between moisture uptake and temperature is quite complex because a change of temperature can result in a change of diffusion coefficient of FRPs. As a result, the rate of moisture uptake may increase or decrease depending on the orientation of temperature changes. (Verghese et al., 1998) In the literature, the results of degradation of mechanical properties of FRPs obtained by different research groups showed a wide range of deviation.

Deicing chemicals

Large amounts of deicing salts are used on bridges during the winter season to control snow and ice. Since FRPs are non-corrosive materials, the deicing chemicals cannot trigger any corrosion damage to the FRPs, though they may have other adverse effects on the fibers, such as degradation of stiffness and strength if the fibers are inappropriately coated and shielded by the resin matrix during the production process. Saadatmanesh and Tannous (Saadatmanesh and Tannous 1997) conducted extensive tests for eight different GFRP rebars by immersing them in three different salt solutions at 25^oC for six months: 3% NaCl, 7% $NaCl+CaCl_2$ (2:1), and 7% $NaCl+MgCl_2$ (2:1). It was found that the vinyl ester provides a better protection against chloride than polyester and aramid do, and that the carbon tendons have a much better resistance to salt attacks than that of E-glass and AR-glass rebars. Gangarao and Vijay (Gangarao and Vijay 1997) observed the strength and stiffness reductions up to 17% for four different GFRP plates with E-glass fibers immersed in a 4% salt solution for 220 to 240 days at room temperature.

Alkali attack

One of the main concerns about the use of FRP products is what the durability in alkaline environments will be, such as the pore solution of concrete. Because of the chemical attack on the glass fibers and because of the concentration and growth of hydration products between individual filaments, the strength and stiffness of FRP materials can be reduced significantly in concrete environments. (Murphy et al., 1999) The durability of FRP materials in the alkaline environment is strongly dependent on resin types and the manufacturing processes. Coomarasamy and Goodman (Coomarasamy and Goodman 1997) conducted tests on different glass fibers containing two types of resin (polyester and vinylester resin). FRP specimens were subjected to an alkaline solution of pH 13.5 at 60^oC for eleven weeks. The tensile strength reduction of the polyester type specimens was over a wide range from 7 ~ 80%, and the vinylester type had a tensile strength reduction of 45%. It was shown that GFRPs with polyester resin formed a gel-like material which swelled, followed by blistering and disintegration of the resin. Uomoto et al. (Uomoto et al., 1997) conducted a durability test on GFRPs submerged in a

$Na(OH)_2$ solution at 40^oC for 120 days. GFRP specimens experienced a reduction of tensile strength of up to 70%.

Ultraviolet light

FRPs may be degraded by weathering effects, particularly by ultraviolet (UV) light. Ultraviolet photons from the natural solar radiation cause photo-oxidative reactions that can alter the molecular chain of polymers and produce microcracking in the polymer. Thus, UV radiation can deteriorate the durability of GFRP. (Singh et al.) In order to investigate the influence of ultraviolet light on FRPs, Rahman et al. (Rahman et al. 1998) conducted some tests on IM7/997 carbon/epoxy composite laminates. A 9% reduction in the transverse strength was evidenced after 1000 hours of exposure to ultraviolet radiation. Surface microcracking and chemical degradation of the epoxy were observed. Sasaki et al. (Sasaki et al., 1997) reported a 40% reduction in the tensile strength of FRPs after exposure to sunshine for 42 months. Kato et al. (Kato et al 1997) conducted the test using ultraviolet rays on GFRP rods for 1250 exposure cycles (102 minutes in dry condition and 18 minutes in wet condition). An 8% reduction in the tensile strength was measured at the 0.2MJ/m^2 ultraviolet radiation intensity.

1.3 Experimental Plan

The objectives of the experimental study were to assess the effects of the above mentioned environmental conditions on mechanical properties of GFRPs, specifically on Young's modulus and tensile strength of the selected GFRP. In this study, the modulus of elasticity (in psi units) is taken as the highest slope of straight line from initial point of the stress-strain curve. The tensile strength of the material is calculated by dividing the maximum applied load by the initial undeformed cross-sectional area of the specimen.

1.3.1 Specimen preparation

The GFRP laminated plates were provided by Kansas Structural Composites, Inc. The plates were cut into small pieces in rectangular shapes by the company. Vinylester was used for matrix material of the specimens. The average width, length and thickness of the specimens are 0.96 in, 9.0 in and 0.14 in, respectively.

1.3.2 Conditioning of specimens

Prior to the testing of specimens for the mechanical properties, the specimens were pretreated by subjecting them to various environmental conditions. This process, referred to as the conditioning of the specimens, is designed to generate deterioration of GFRP materials similar to that experienced in a service environment. After the GFRP specimens were conditioned, the mechanical properties of the conditioned GFRP specimens were evaluated and compared to the GFRP specimens without the conditioning.

Freeze-Thaw Cycles

ASTM C666 (Standard Test Methods for Resistance of Concrete to Rapid Freezing Thawing) was used in the present study for the freeze-thaw conditioning of GFRP specimens, although the testing procedures specified by ASTM C666 were originally designed for the durability of concrete. An environmental chamber manufactured by Russells Technical Products was used for the freeze-thaw conditioning. It is shown in Figure 1.

Figure 1. The environment chamber used in the project

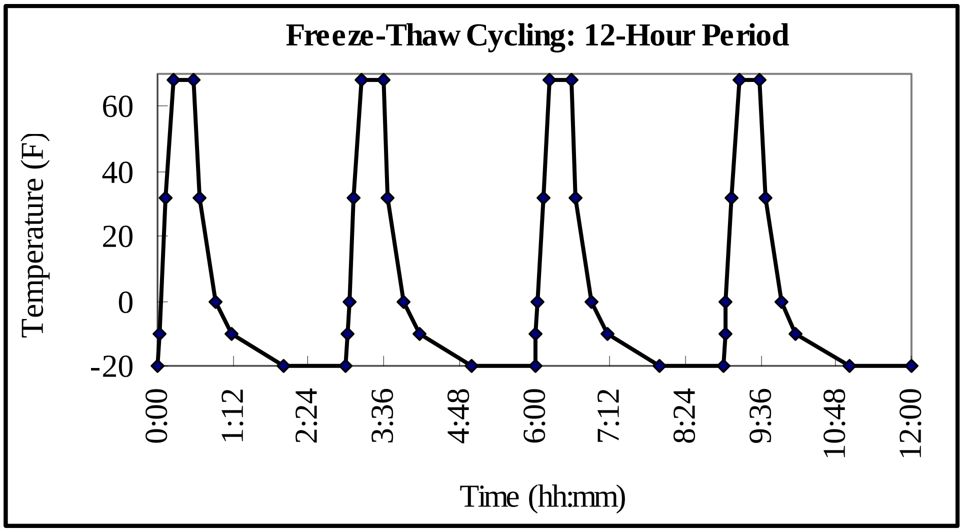

Figure 2. Freeze-thaw cycling program for a 12-hour period

The specimens were subjected to a temperature variation ranging between -20°F(-29°C) to 68°F(20°C), over 8 cycles per day with an one hour hold at -20°F and a 20-minute hold at 68 °F. Figure 2 shows the temperature cycles graphically for a 12 hour period. The specimens were exposed to 300 total freeze-thaw cycles (750 total hours of exposure).

Wetting and Drying Cycles

In order to investigate the effects of wetting/drying cycles on the durability of the GFRP, two specimens were immersed in a water bath at room temperature for 30 minutes, then pulled out of the bath and hung in the air for 30 minutes. The wetting/drying cycles were repeated 2,160 times over 90 days. The testing apparatus is shown in Figure 3.

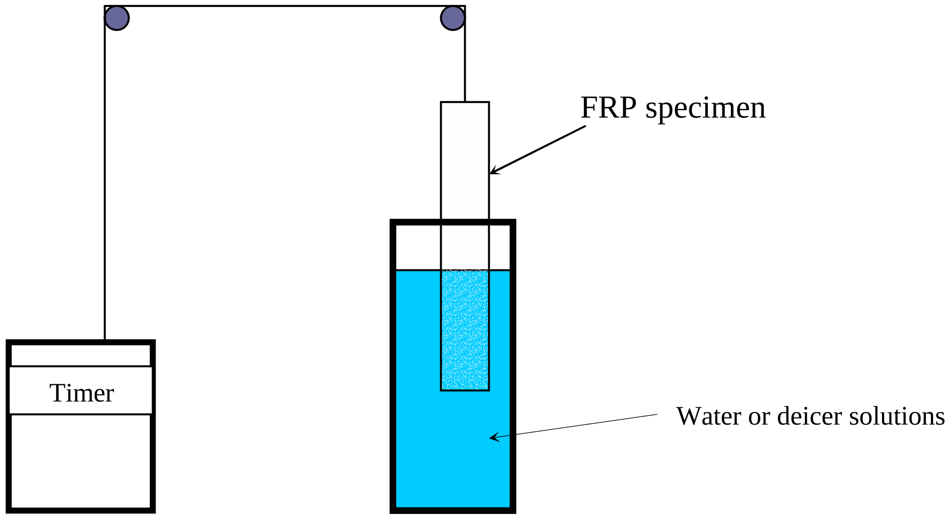

Figure 3. The wetting and drying apparatus

Deicing Chemicals

The influence of deicing chemicals such as magnesium chloride ($Mg(Cl)_2$), calcium chloride ($Ca(Cl)_2$), and sodium chloride (NaCl) on the behavior of FRP materials was investigated. Both long-term ponding tests and long-term cyclic wetting/drying tests in the chloride solutions were carried out. For the ponding test, a total of 15 specimens were immersed in the solutions of three deicing chemicals. The deicer solutions were $Mg(Cl)_2$ of 3%, $Ca(Cl)_2$ of 3%, and NaCl of 3%. The ponding tests were continued at room temperature for 90 days, as shown in Figure 4. For the cyclic wetting/drying test in the chloride solutions, a total of 12 specimens were tested using the same apparatus shown in Figure 3. The three different solutions of the deicing chemicals were used in the bath instead of water.

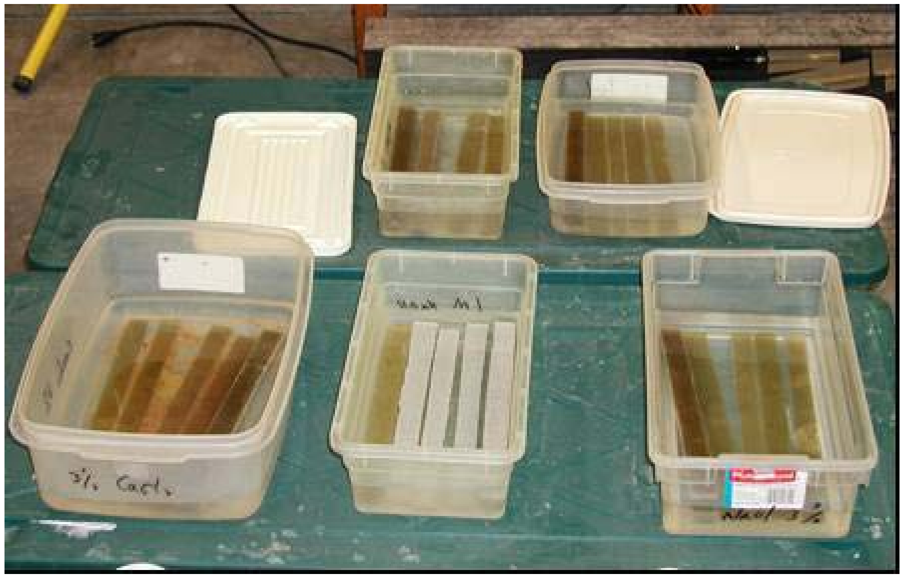

Figure 4. Immersion of FRP specimens in three solutions of deicing chemicals

Alkaline and Acid Attack

Alkaline and acid attacks to GFRPs were simulated by using sodium hydroxide solution (1M NaOH) and hypochloric acid (1M HCl). A total of 4 specimens were submerged in the alkali and acid solutions respectively for 90 days at room temperature in the same manner as shown in Figure 4.

Ultraviolet Radiation

A standard ultraviolet (UV) resistance test based on ASTM G53 was used to simulate the weathering effect, particularly the deterioration of GFRPs caused by sunlight. The testing cycles are specified in ASTM D 5208. Three specimens were exposed to the cyclic fluorescent ultraviolet radiation in an environmental chamber for 90 days based on the Cycle C procedure of ASTM D 5208. The temperature in the chamber was kept at 50°C. The test chamber and the ultraviolet light are shown in Figure 5.

Figure 5. Ultraviolet Radiation Apparatus

Figure 6. Experimental setup for uniaxial tension test of a GFRP specimen

1.3.3 Uniaxial tension tests

The uniaxial tension test was carried out after the conditioning of the specimens was complete in order to investigate the degradation of the GFRPs exposed to environmental conditions. The uniaxial tension tests were performed on a Series 10,000 Bench UTM (Tinius Olsen Machine), as shown in Figure 6. The machine was equipped with a 10,000 lb load-cell. The specimens were inserted between the two grips of the testing machine and then loaded in tension until fracture occurred. To prevent any possible slip during loading, lateral pressure was applied at the grips. The tensile load was applied in the longitudinal direction, as shown in Figure 6. The specimens were subjected to uniaxial loading in tension with a displacement rate of 10 in/min. The load P and the elongation of the specimens were recorded. After the nominal stress and nominal strain were calculated, the Young's modulus and the tensile strength of the specimens were obtained.

1.4 Experimental Results

(1) Failure pattern

All GFRP specimens failed in a very brittle manner under uniaxial tensile loading, as shown in Figure 7. The explosive failure occurred at the midpoint of the specimens. The failure pattern was consistent for all GFRP specimens with and without the environmental conditioning.

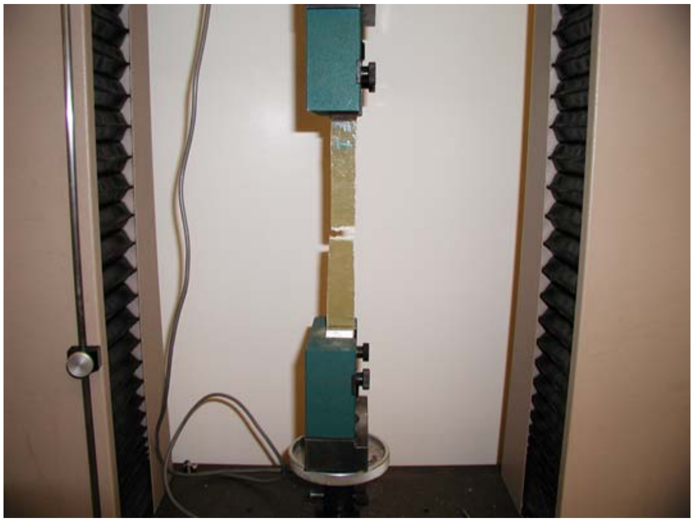

Figure 7. The failure mode of a GFRP specimen

(2) The influence of freeze-thaw cycles

The specimens were subjected to 300 freeze-thaw cycles totaling 750 hours of exposure with the temperature ranging from 20°F (-29°C) to 68°F (20°C). Figure 8 shows the tensile stress-strain response of the GFRP specimen after the freeze-thaw cycling test.

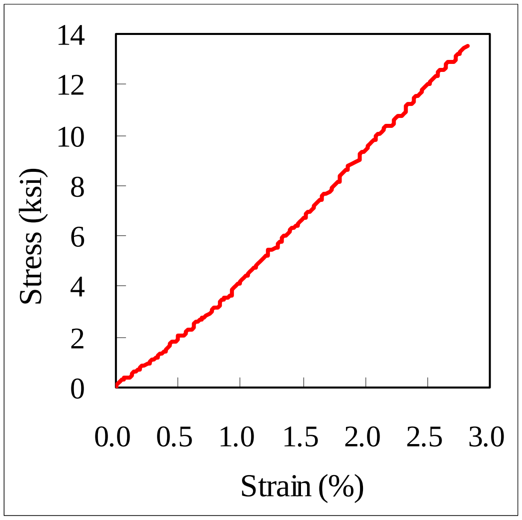

Figure 8. Tensile stress-strain curves of a GFRP bar after the free-thaw cyclic testing

The stress-strain curve of the GFRP specimen maintained a nearly linear progression up to the failure point.

The Young's modulus of the GFRP specimens was reduced by 18% after the freeze-thaw conditioning, and the tensile strength was reduced by 10%, as shown in Table 1. The reduction in Young's modulus could be induced by the thermal fatigue.

The controlled GFRP bar exposed to room temperature at 78.8^{o}F and relative humidity at 35% is used for the comparison of mechanical properties. The degraded tensile strength and Young's modulus of the controlled GFRP bar were 15 ksi and 1074.4 ksi, respectively.

Table 1. Mechanical properties of GFRP specimens after the freeze-thaw cyclic testing

Condition	Ultimate Tensile Strength (ksi) [Reduction (%)]	Young's Modulus (ksi) [Reduction (%)]
Controlled	15.1	1074.4
Freeze-Thaw	13.5 [10]	878.1 [18]

(3) The influence of wetting/drying cycles in water

After 90 days of wetting/drying conditioning, the Young's modulus and tensile strength of the GFRP specimens were reduced by 4% and 27%, respectively, as shown in Table 2.

Table 2. Mechanical properties of GFRP specimens after wetting/drying cycles in water

Condition	Ultimate Tensile Strength (ksi) [Reduction (%)]	Young's Modulus (ksi) [Reduction (%)]
Controlled	15.1	1074.4
Water wetting/drying condition	14.5 [4]	785.47 [27]

The stress-strain curve of the GFRP specimen after wetting/drying cycles in water is shown in Figure 9.

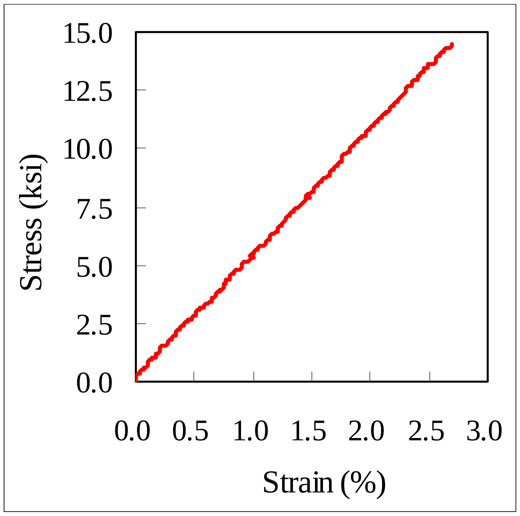

Figure 9. A tensile stress-strain curve of a GFRP specimen after wetting/drying cycles in water

(4) The influence of deicing chemicals (the Ponding Test)

After the ponding test of the three deicing chemical solutions, the tensile strengths of the GFRP specimens were reduced significantly ranging from 12% to 16%, as shown in Table 3.

Table 3. Mechanical properties of GFRP specimens exposed to deicing chemicals (Ponding Test)

Condition	Ultimate Tensile Strength (ksi) [Reduction (%)]	Young's Modulus (ksi) [Reduction (%)]
Controlled	15.1	1074.4
$Mg(Cl_2)$ 3%	13.2 [13]	797.5 [26]
$Ca(Cl_2)$ 3%	13.2 [12]	850.2 [21]
NaCl 3%	12.7 [16]	768.8 [28]

The reductions of Young's modulus were significant, from 21% to 28% as shown in Table 3. In terms of each individual deicer, NaCl has the strongest effect on the tensile strength of GFRP specimens, which is 16%, and the strongest effect on Young's modulus, which is 28%. The ultimate tensile strengths and Young's modulus exposed to each deicing chemicals are compared in Figure 10.

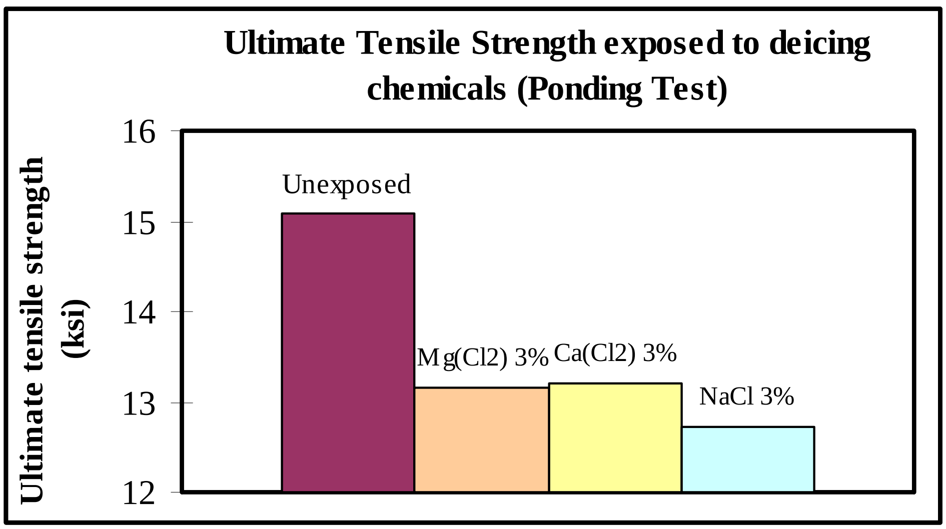

(a)

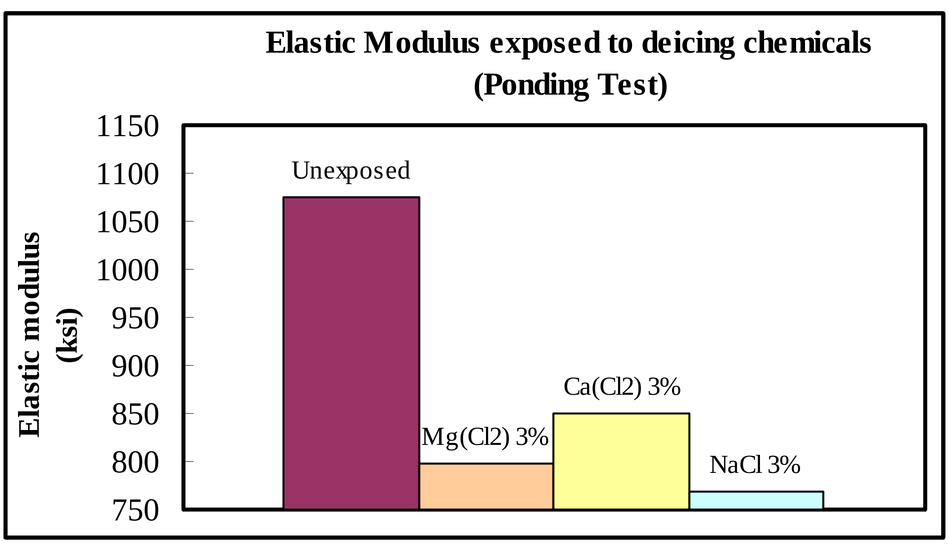

(b)

Figure 10. Comparison of mechanical properties of GFRP specimens exposed to deicing chemicals (the ponding test) (a) Ultimate tensile strength; and (b) Young's modulus

(5) The influence of deicing chemicals (Cyclic wetting/drying test)

Long-term durability tests were conducted for GFRP specimens cyclically exposed to the three deicing salts: $Mg(Cl_2)$ 3%, $Ca(Cl_2)$ 3%, and NaCl 3%. The results of the experiments are shown in Table 4.

Table 4. Mechanical properties of a GFRP bar exposed to deicing chemicals (Cycling test)

Condition	Ultimate Tensile Strength (ksi) [Reduction (%)]	Young's Modulus (ksi) [Reduction (%)]
Controlled	15.1	1074.4
$Mg(Cl_2)$ 3%	13.4 [11]	773.1 [28]
$Ca(Cl_2)$ 3%	14.7 [2]	726.5 [32]
NaCl 3%	11.5 [24]	768.8 [28]

The reductions of Young's modulus by cyclic exposure of deicing chemical were more significant than ponded exposure, from 28% to 32% as shown in Table 4. In terms of each individual deicer, NaCl has the strongest effect on the tensile strength of GFRP specimens, which is 24%; $Ca(Cl_2)$ has the strongest effect on Young's modulus, which is 32%. The ultimate tensile strengths and Young's modulus exposed to each deicing chemicals are compared in Figure 11.

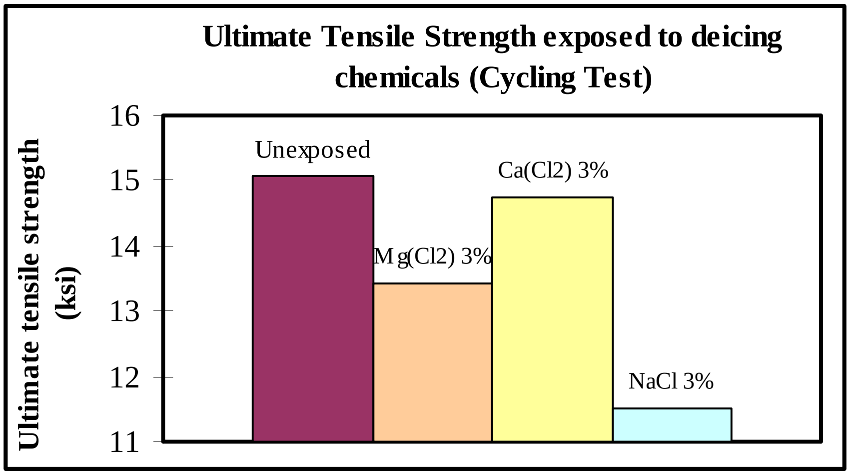

(a)

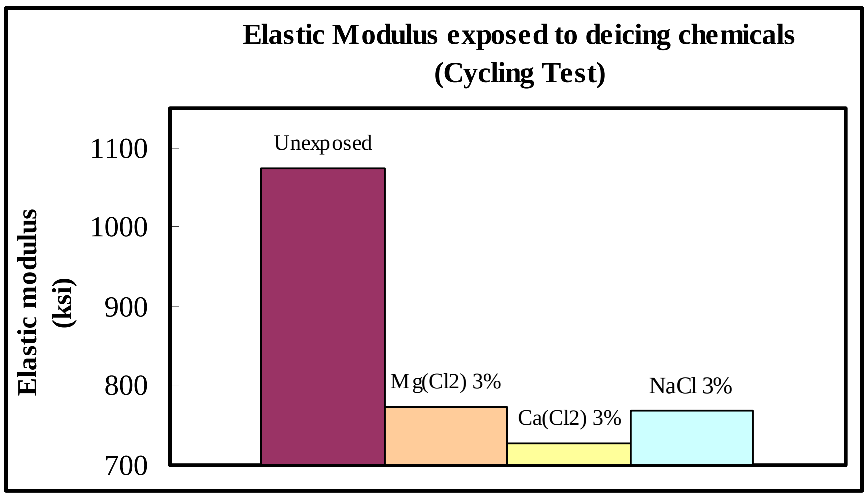

(b)

Figure 11. Comparison of mechanical properties of a GFRP bar exposed to deicing chemicals (Ponding test) (a) Ultimate tensile strength; and (b) Young's modulus

The influence of alkaline and acid attack

The exposure of the GFRP bar to 1M NaOH resulted in a decrease in tensile strength of 35% and a decrease of 28% in the Young's modulus as shown in

Table 5. The tensile strength and Young's modulus were reduced up to 6% and 25% by the acid attack (1M HCl). Based on the test results, the tensile strength of the GFRP bar was not seriously

reduced, but a 25% reduction in Young's modulus was observed by the exposure of 1M HCl acid attack, shown in
Table 5.

Table 5. Mechanical properties of GFRP specimens exposed to alkaline attack

Condition	Ultimate Tensile Strength (ksi) [Reduction (%)]	Young's Modulus (ksi) [Reduction (%)]
Controlled	15.1	1074.4
1M NaOH	9.8 [35]	773.9 [28]
1M HCl	14.1 [6]	804.02 [25]

The influence of ultraviolet radiation

To investigate the influence of cyclic sunlight exposure to the GFRP, an ultraviolet radiation test was conducted. A considerable reduction in both the tensile strength and Young's modulus as a result of ultraviolet radiation was observed. The reduction for tensile strength was 22% and the Young's modulus was reduced by 29%. The results are listed in Table 6.

Table 6. Mechanical properties of GFRP bar exposed to ultraviolet radiation

Condition	Ultimate Tensile Strength (ksi) [Reduction (%)]	Young's Modulus (ksi) [Reduction (%)]
Controlled	15.1	1074.4
Ultraviolet Radiation	11.7 [22]	763.9 [28]

1.5 Suggestions for Future Research

Experimental results were obtained in this study for a systematic assessment of long-term durability behaviors of GFRP, specifically the extent of strength reduction and stiffness reduction of GFRPs under various simulated service environments. The information is very important for bridge design engineers, contractors, and state transportation agencies for the selection, construction, and maintenance of FRP materials used in bridge structures. It is important to note that the present study did not intend to investigate specific deterioration mechanisms of GFRPs that are responsible for the strength and stiffness reductions under the testing environments. From the material science and material engineering points of view, more studies are needed to investigate the changes of chemical composition and the microstructure of the GFRP materials caused by the environmental parameters, which is absolutely important for further improving the performance of the GFRPs, as well as for developing new materials.

For the ponding test, the weights of specimens before and after ponding should be measured and compared. This is important evidence for measuring the moisture intake capacity of the GFRP specimens.

The accelerated testing environments should be correlated with actual environmental conditions. For example, the testing environment should be created so that the number of months or years of applications of deicing salts is equivalent to a one-month period of 3% NaCl solution cyclic wetting/drying conditioning. This is not an easy task, but will be very useful for practical applications.

2. In-situ Monitoring of the GFRP Deck Panel

2.1 Introduction

In May 2003, the O'Fallon Park Bridge was built over Bear Creek in Denver Mountain Parks in the state of Colorado. The bridge is 41'-3 7/16" long and about 16' wide. The new bridge is composed of six GFRP honeycomb composite deck panels of 16' 3" length and 7'-31/2" width. The FRP Honeycomb (FRPH) panels were constructed by Kansas Structural Composites, Inc (KSCI) and are shown in Figure 12.

Figure 12. Fiber-Reinforced Polymer Honeycomb (FRPH) Sandwich Panels

The bridge was designed by ASSHTO LRFD Bridge Design Specification (1998) with Interim Specifications, City & County of Denver Standard Specifications (1999), Colorado DOT Standard Specifications (1999), and ACI 440.1R-01 "Guide for the Design and Construction of Concrete Reinforcement with FRP Bars." The bridge is designed for Type 3 Colorado Posting Vehicle with Impact Factor 10%. (The bridge is capable of supporting an AASHTO HS-25 load, 1, 500, 000 pounds). Permanent fiber optic sensors were embedded into Panel 6 during the manufacturing of the panels. A plan view and the dimensions of the bridge are sketched in Figure 13. Design details can be seen in Reference 21.

A load test using a CDOT dump truck was performed on the bridge on August 20, 2003 to evaluate the behavior of the bridge deck panel. Strains in the panel were measured for four static load cases and temperature effect on the FRPH panels to monitor the performance of the bridge. Strains were also measured on February 17, 2004 for the temperature effect.

Figure 13. The bridge in O'Fallon Park, Denver, Colorado

2.2 Installation of Fiber Optic Sensors

Due to their high accuracy, small size, fast response, non-electric (immunity to electromagnetic and radio-frequency interference) and lightning surcharges, fiber optic sensors (strain gages) were applied to monitor structural responses of a FRPH panel at the O'Fallon Park Bridge. A typical fiber optic sensor can be seen in Figure 14.

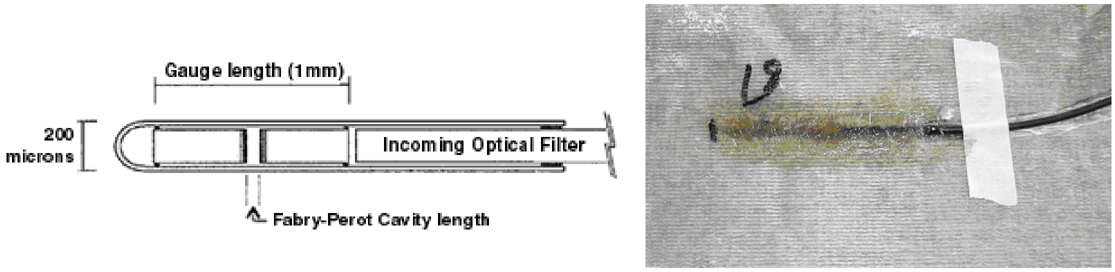

Figure 14. Fiber optic strain gage

A Fabry-Perot fiber optic strain sensor was chosen in the project. When a gage is bonded to a substrate, a strain variation in the axial direction of the strain gage will produce a variation of the cavity length, which can be converted into a numerical strain value. A total of twenty strain sensors were embedded at Panel 1 (seen in Figure 13) longitudinally and transversely so that various load effects could be observed, including dead loads, live loads, snow loads and wind loads. The gages were permanently installed as shown in Figure 15 so that long-term effects due to settlement and creep can also be monitored over time. The detail of placement of fiber optic sensors on the panel is shown in Figure 16.

Figure 15. Installation of fiber optic sensors in the FRPH panel

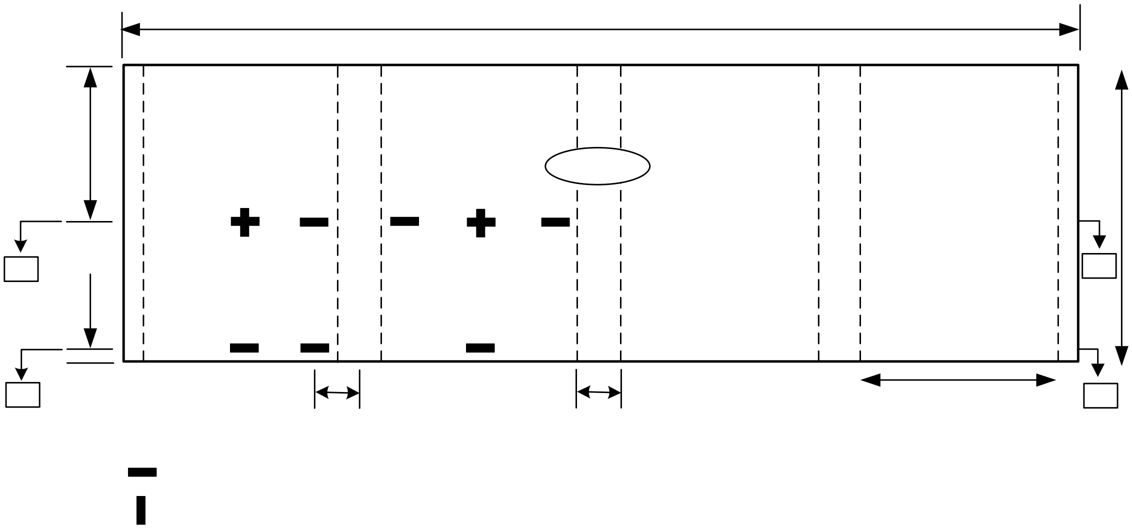

(a) Top view (Panel 1)

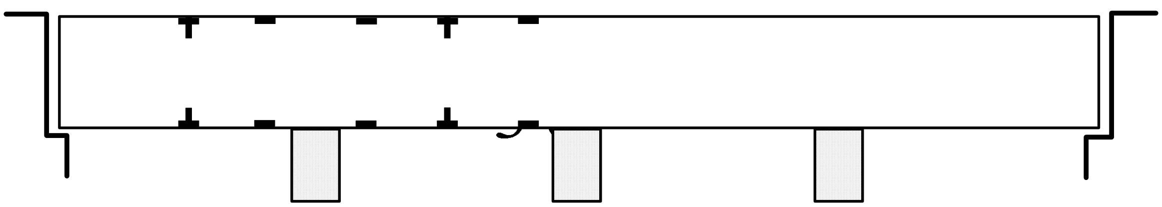

(b) A-A Plan view

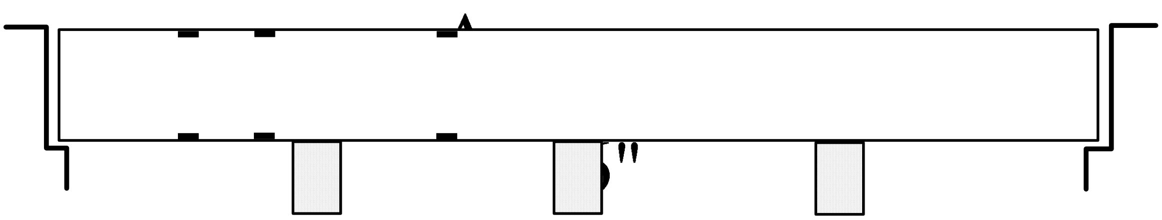

(a) B-B Plan view

B

Figure 16. The locations of fiber optic sensors in the FRPH panel

9

: Strain gage in di

The monitoring system is illustrated in Figure 17. The fiber optic cables were used to connect the sensors with the digital logger called DMI Multi-Channel Fidel Data Logger. The readout in terms of strain values can be displayed directly on the Window-based data acquisition software called FISO Software.

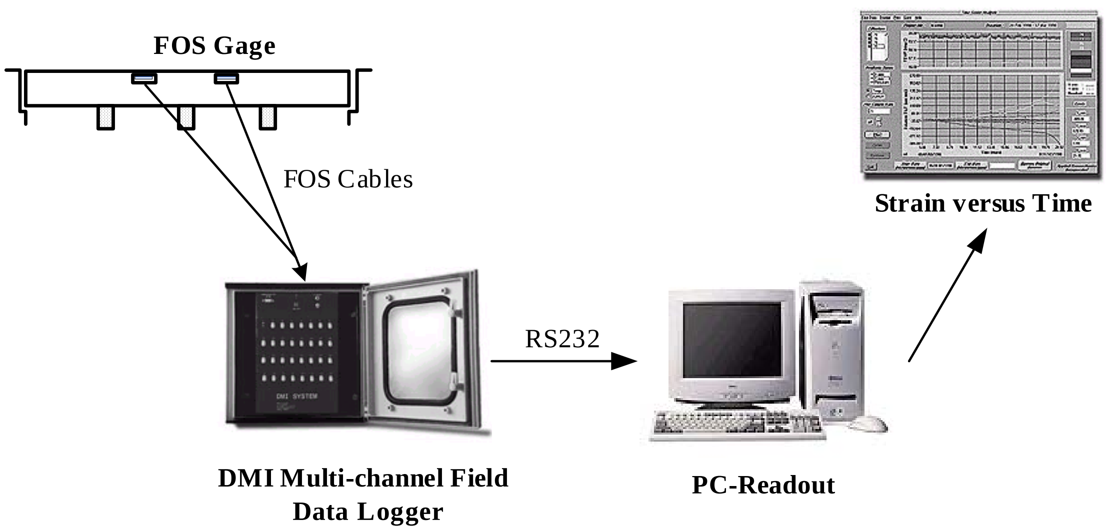

(a) The data acquisition system

(b) The ditch for embedding fiber optic cables

(c) The data logger

Figure 17. Installation of the fiber optic strain gage monitoring system

2.3 In-situ Monitoring of the Bridge Decks

2.3.1 Results of truck loading test

A loading test was performed using an empty CDOT dump truck to determine the FRPH deck panel behavior for the actual live load, as shown in Figure 18.

(a) Front view of the loading truck

(b) Back view of the loading truck

Figure 18. Load test for the bridge (a CDOT dump truck)

The axle loads of both the front axle and rear axle are provided in Figure 19.

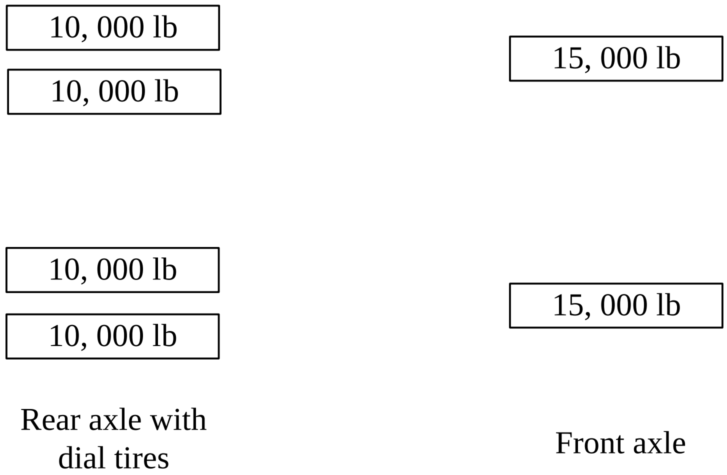

Figure 19. The axle load of the CDOT truck

The strains were recorded in twenty channels both in the longitudinal and lateral directions. Data were collected with an acquisition rate of 3 seconds and acquisition average interval of 0.05 seconds. Four load cases were performed to measure strains at the top and bottom of the FRPH panel. The truck was positioned so that only the rear axle with dial tires was located on the desired locations. Once the truck was positioned, strains were recorded. The readings were also taken before the load was applied and used as the reference strains.

Case 1: Loading at Section A-A on the shoulder

For the loading test 1, the rear axle of the truck was loaded at the location shown in Figure 20. Figure 21 shows the microstrain distributions in Section A-A (see Fig. 16).

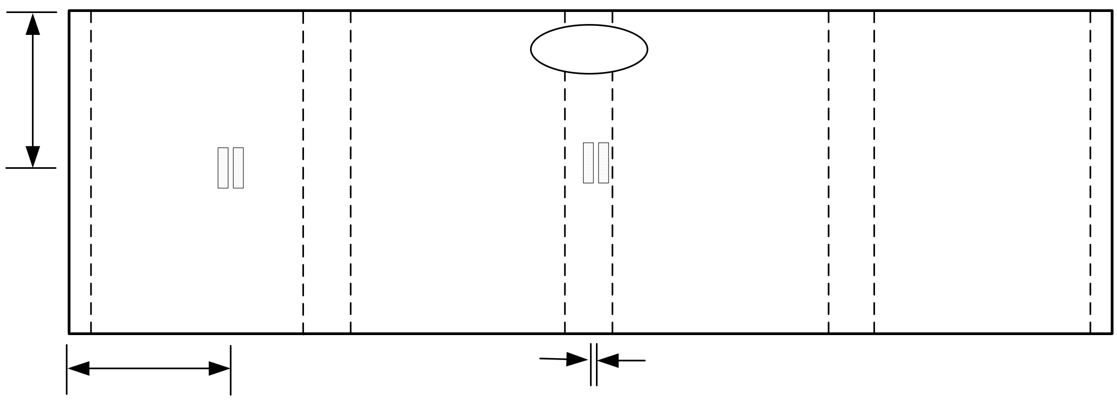

Figure 20. The location of the rear axle in the loading test 1

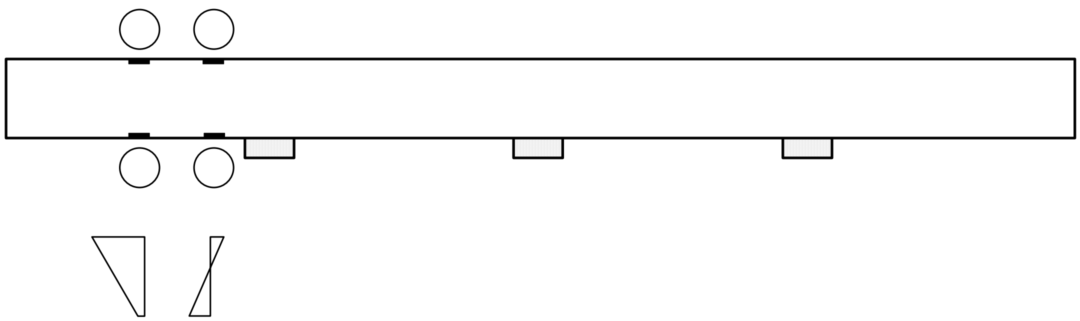

Figure 21. Microstrain distributions in Section A-A

3'

Case 2: Loading at Section B-B on the shoulder

For the loading test 2, the rear axle of the truck was loaded at the location shown in Figure 22. Figure 23 shows the microstrain distributions in Section B-B (see Fig. 16).

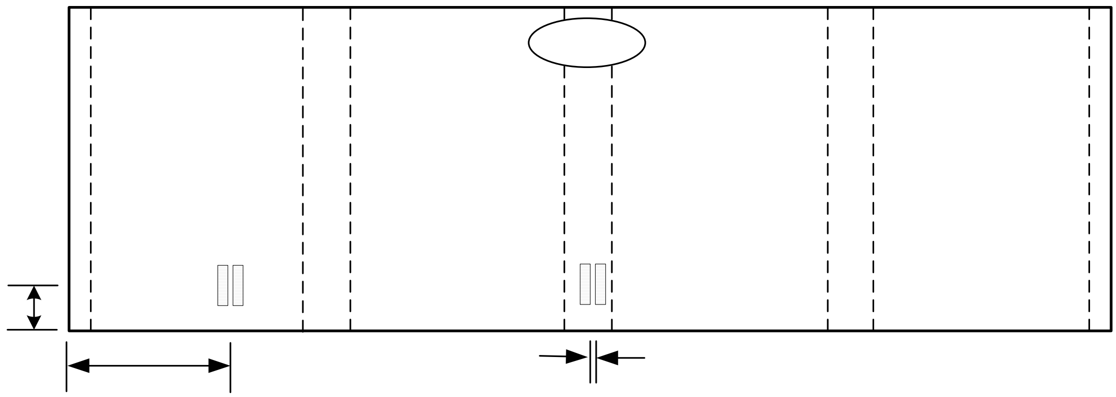

Figure 22. The location of the rear axle in the loading test 2

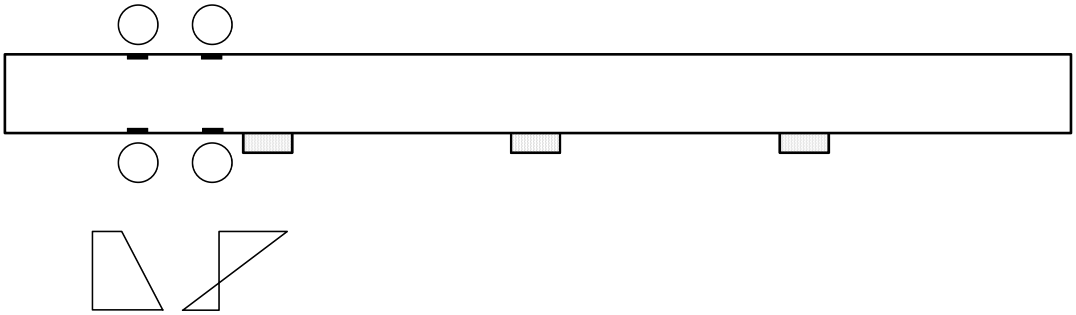

Figure 23. Microstrain distributions in Section B-B

Case 3: Loading at Section A-A in the midspan

For the loading test 3, the rear axle of the truck was loaded at the location shown in Figure 24. Figure 25 shows the microstrain distributions in Section A-A (see Fig. 16).

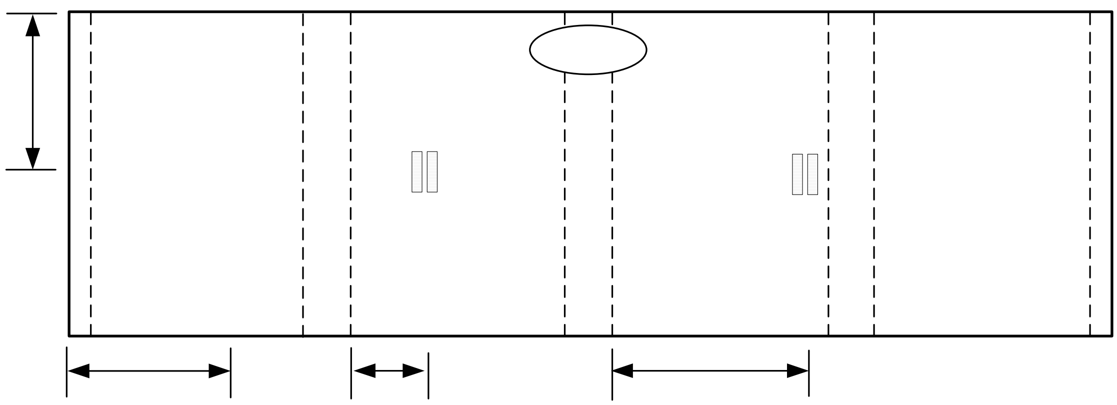

Figure 24. The location of the rear axle in the loading test 3

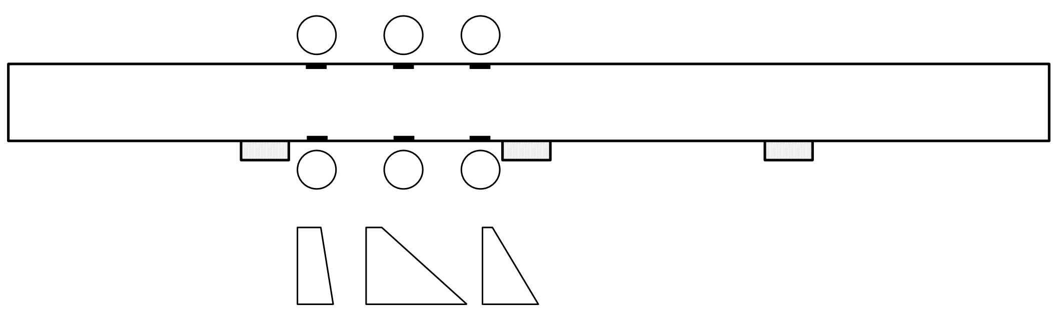

Figure 25. Microstrain distributions in Section A-A

3' 5"

Case 4: Loading at Section B-B in the midspan

For the loading test 4, the rear axle of the truck was loaded at the location shown in Figure 26. Figure 27 shows the microstrain distributions in Section B-B (see Fig. 16).

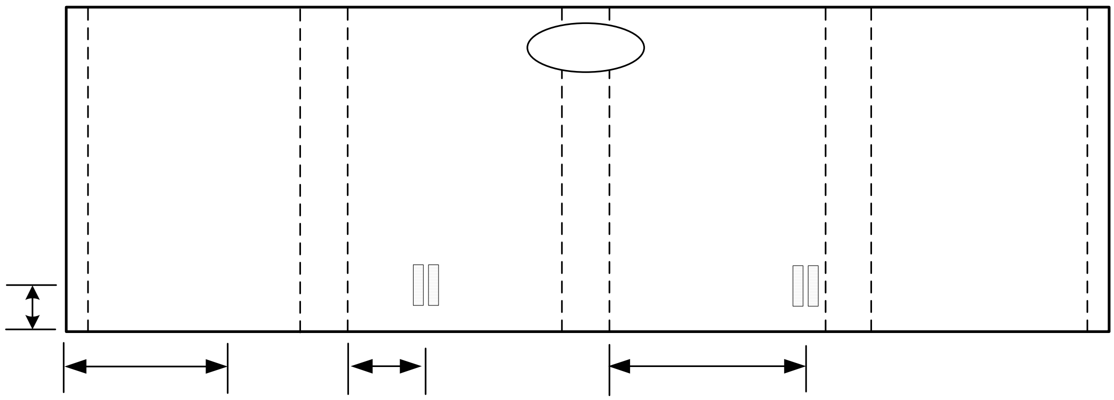

Figure 26. The location of the rear axle in the loading test 4

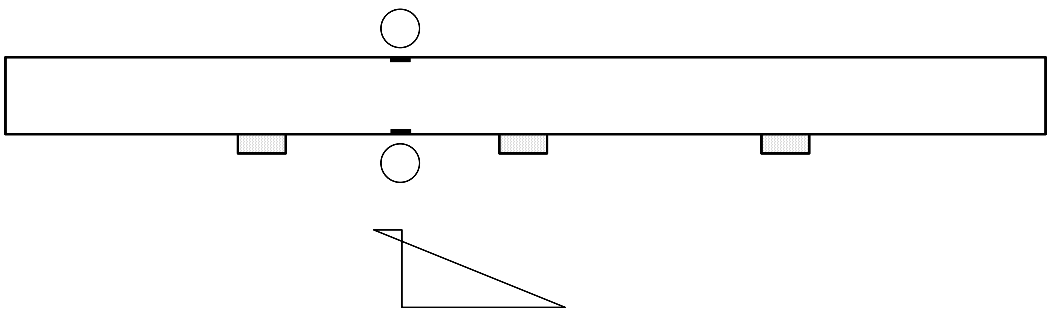

Figure 27. The microstrain distribution in Section B-B

2.3.2 Temperature effect

The FRPH panels are subjected to significant variations of environmental conditions during the initial fabrication process and the service period. Among the many environmental conditions, temperature effect is a very important one. To monitor the effect of temperature variation on the internal strain/stress of the panel, two readings were taken, one in the summer and one in the winter. The strains were measured continuously for 110 minutes from 9:30 a.m. to 11:10 a.m. on September 12, 2003 and for 120 minutes from 10:00 a.m. to 12:00 p.m. on February 17, 2004. Temperatures were measured from the top surface and the bottom surface of the panel. The temperature readings of the top surface were taken in the wearing surface (gravel overlay, 1/2"), and the temperatures of the bottom surface were taken from underneath the precast concrete arch near the sensor locations. The temperature profiles are shown in Figure 28, and the strain variations are shown in Figures 29, 30, and 31.

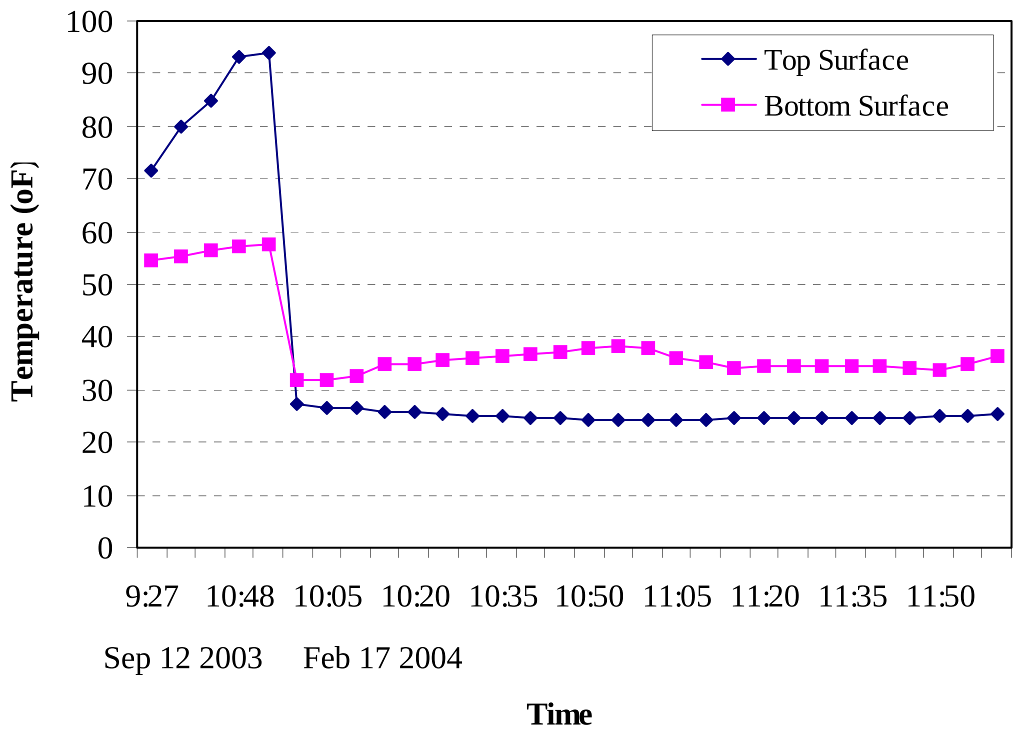

Figure 28. Temperature profiles at the top and bottom surfaces of the panel (September 12, 2003 and February 17, 2004)

In Figure 28, the surface temperature is higher than the bottom temperature in the summer, which is due to the direct, heavy sunshine in the summer. The surface temperature is lower than the bottom temperature in the winter, which is due to the relatively stagnant air under the arch of the bridge, and there is no direct cold wind.

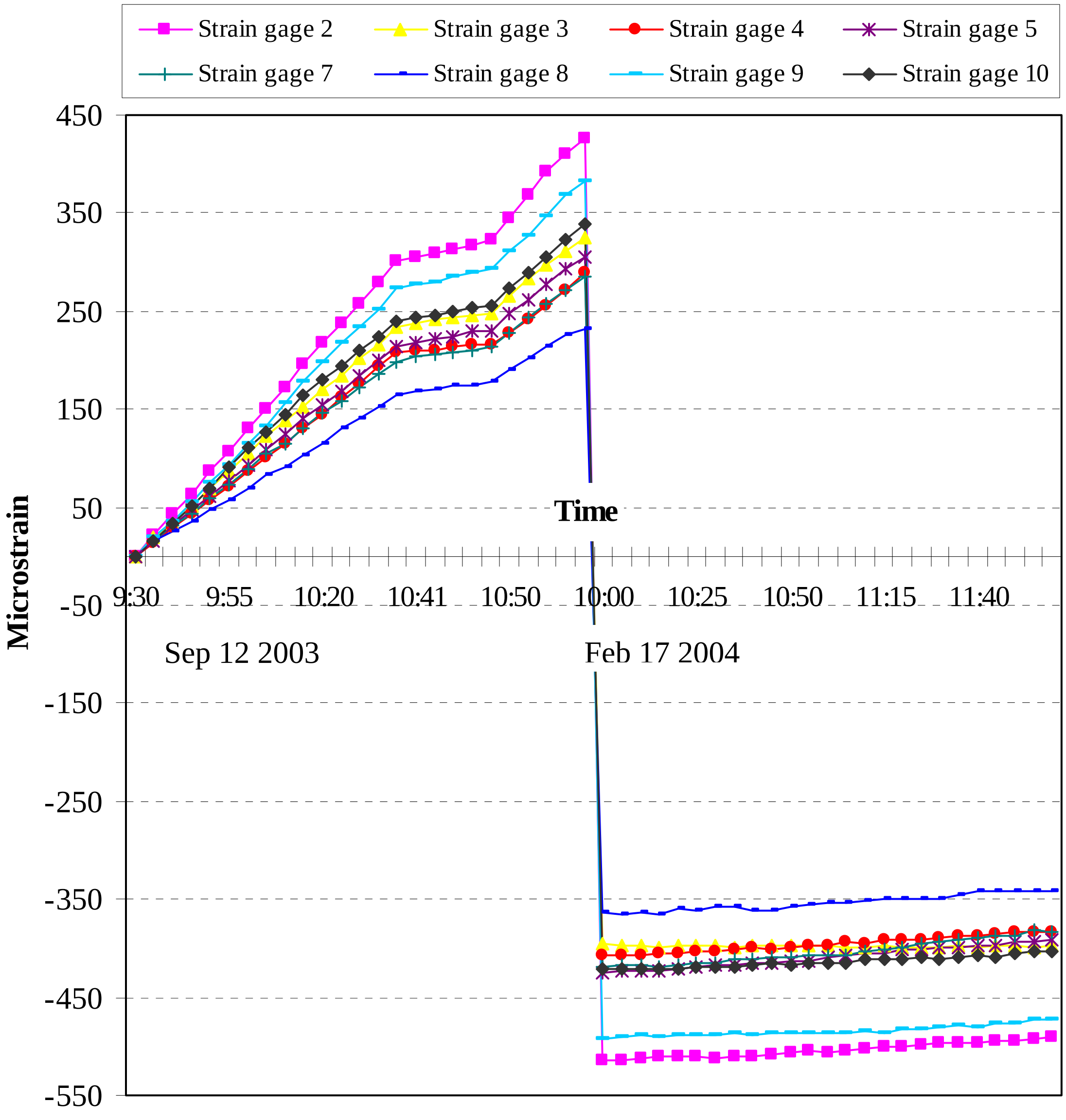

Figure 29. Longitudinal microstrains versus time in the top of the panel due to the temperature effect

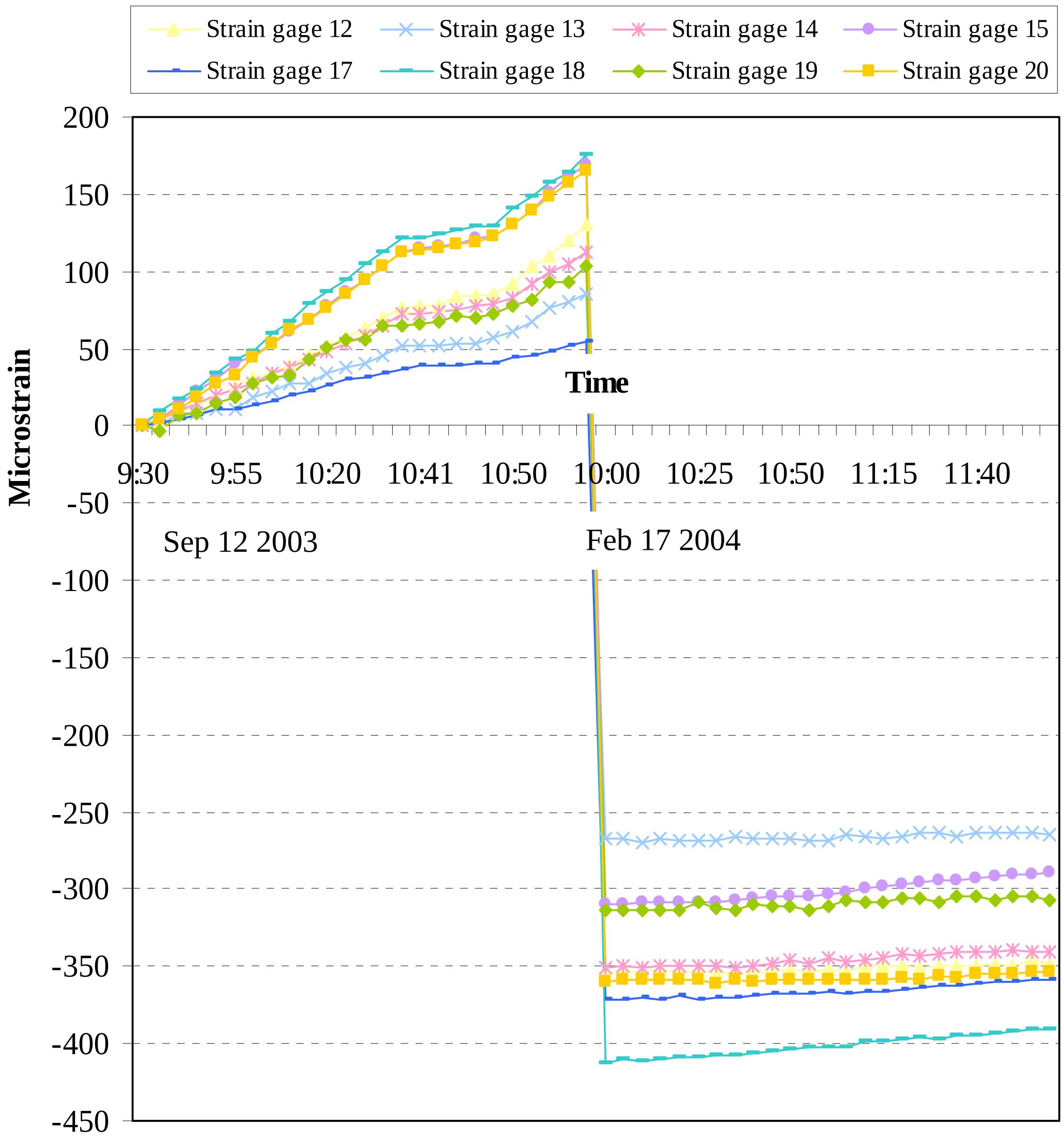

Figure 30. Longitudinal microstrains versus time in the bottom of the panel due to the temperature effect

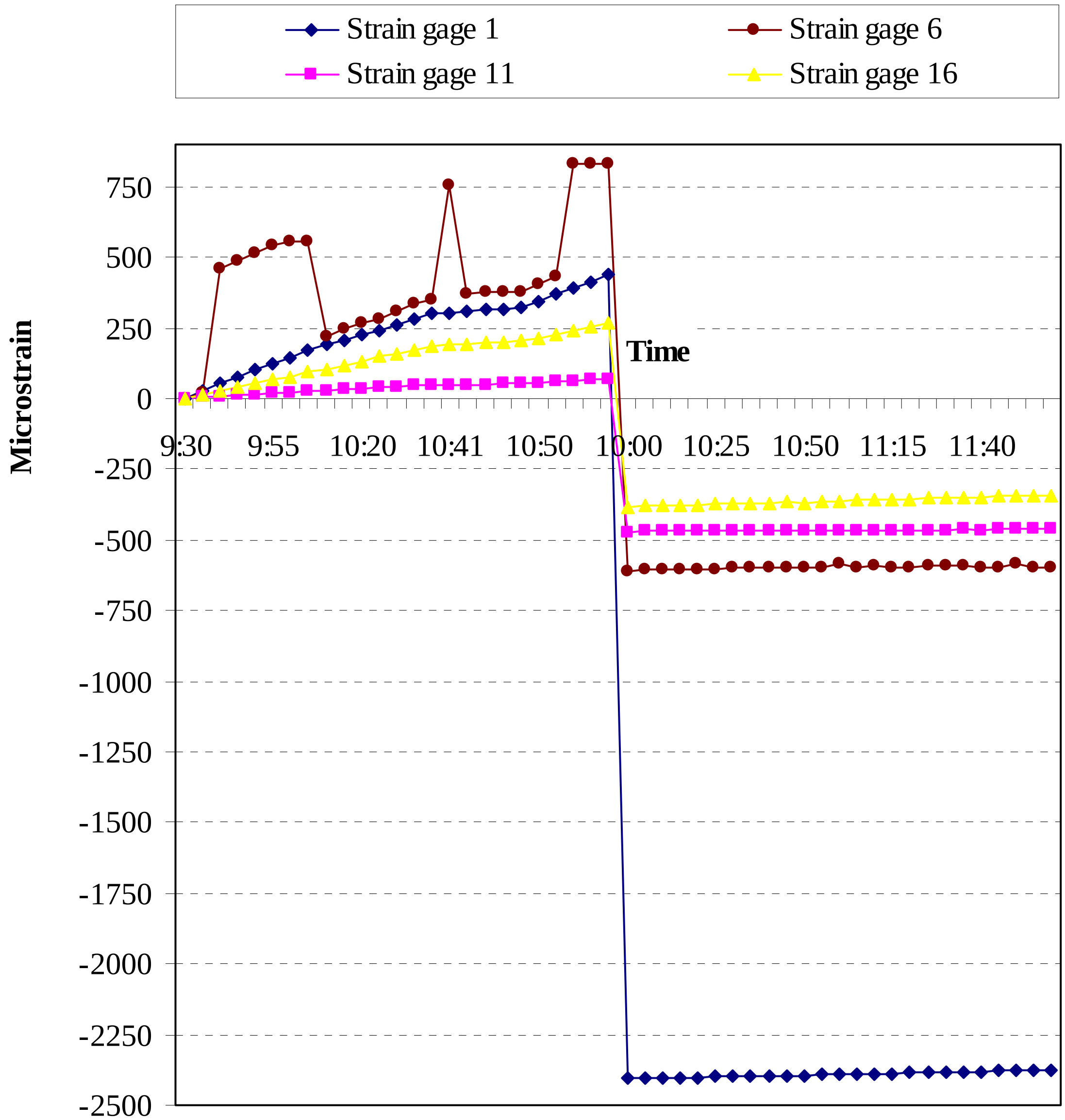

Figure 31. Transverse microstrains versus time in the panel due to the temperature effect

In Figure 31, the strains from gage 6 in the summer, and the strains from gage 1 in the winter look abnormal. Taking the gage 1 as an example, the strains of gage 1 during the reading period were quite stable, about 2400 με. Using the Young's modulus of unexposed GFRP specimen, 662 ksi (see Table 5), the corresponding stress is about 1600 psi, which is only about 10% of the ultimate strength of the unexposed specimen. Therefore, the gage 1 may have recorded the actual strain in the location. More readings are needed in the future.

3. Conclusions and Recommendations

3.1 Durability of GFRPs

The effect of environmental conditions on the long-term durability of GFRPs was investigated by systematic durability testing. Several environmental parameters were considered in this study, including freeze-thaw effects, moisture effects (continuous ponding and cyclic wetting/drying), deicing chemicals (continuous ponding and cyclic wetting/drying), alkaline and acid attacks, and natural sunlight exposure (UV light). The degradation of mechanical properties of GFRPs was determined in terms of tensile strength and Young's modulus.

Every environmental parameter tested in the study resulted in a degradation of GFRPs to a certain extent. From the strength aspect, the worst degradation was a 35% reduction of tensile strength of the GFRP subjected to the ponding of 1M NaOH solution. From the stiffness point of view, the worst degradation was a 32% reduction of Young's modulus of the GFRP subjected to the ponding of 3% $Ca(Cl_2)$ solution.

In general, these degradations may be attributed to the chemical reactions in the polymer matrix and microcracks developed in the matrix, as well as in the matrix/fiber interface. In particular, each influential parameter has its own damage mechanism(s) and must be studied separately.

The significant degradations in terms of the tensile strength and the stiffness must be considered in the specifications related to the structural design of bridge decks if the GFRP is to be used widely for bridge decks in the state of Colorado.

For future work, it is suggested that the degradation of FRP should be tested with coupling effects. Due to coupling effects between moisture and elevated temperatures, the degradation could be accelerated by high diffusion rates. Additionally, the freeze-thaw, alkali attack, UV radiation, and moisture can be applied concurrently to see how the combinations of the influential parameters affect the degradation of the FRP specimens. For the ponding test, the weights of specimens before and after ponding should be measured and compared. This is an important factor for measuring the moisture intake capacity of the GFRP specimens.

3.2 Monitoring of the Bridge Deck

The strains due to the mechanical loading are very small. Therefore, the structural design of the FRPH panel for O'Fallon Park Bridge is very conservative.

Comparing the effect of temperature (Figures 21, 23, 25, and 27) with the effect of mechanical loading (Figures 29, 30, and 31), one can see that the effect of temperature is clearly dominant. The maximum strain due to mechanical loading is 226 microstrain in Case 4, while the thermal strains in the winter are all higher than that. This means that the temperature variation is more important than the variation of mechanical loading. Therefore, in addition to the mechanical fatigue loading test performed in this project, a larger scale cyclic temperature test for the FRPH panel is very necessary and important for evaluating the long-term performance of the panel.

In the summer when the temperature rose from 70 °F to °95 F in about two hours, all gages showed increasing strain in tension in both longitudinal and transverse directions, which reflects the rapid thermal expansion. While in the winter, when the temperature stabilized on the top and bottom surfaces in the two-hour reading period, all gages showed large strains in compression in both directions, which is the result of thermal contraction. It should be noted that the strains are relative values based on the installation condition (taking the initial strains as the reference readings).

Strain gage 1 showed abnormal readings with very high compressive strain in the winter, compared with other strain gages. It may be due to a problem with the gage, or it may reflect the actual strain at the location. Future readings will confirm the condition of the gage.

The monitoring process of the bridge deck should be continued. The results obtained so far provide valuable information and can be compared to the strains that will be collected in the future to evaluate the long-term performance of the bridge deck.

4. References

Bank L. C., Gentry T. R,, Barkatt A., Prian L., Wang F., Mangla S. R. (1998) “Accelerated Aging of Pultruded Glass/Vinyl Ester Rods,” Fiber Composites in Infrastructure, *Proceedings of the Second International Conference on Fiber Composites in Infrastructure ICCI*, 2, 423-437.

Camat, G., and Shing, P.B. (2004) "Evaluation of GFRP Deck Panel for the O’Fallon Park Bridge," *CDOT Research Report*, Report No. CDOT-DTD-R-2004-02.

Coomarasamy A. and Goodman S. (1997) “Investigation of the Durability Characteristics of Fiber Reinforced Plastic (FRP) Materials in Concrete Environment,” *Proceedings of the American Society for Composites-12th technical conference.*

Dutta, P. K. (1998) “Structural Fiber Composite Materials for Cold Regions,” *Journal of Cold Regions Engineering*, 3(2), 124-132.

Gangarao H. V. S., Vijay P. V. (1997) “Aging of Structural Composites under Varying Environmental Conditions,” Non-Metallic (FRP) Reinforcement for Concrete Structures, *Proceedings of the 3rd International Symposium*, 2, 91-98.

Hayes M. F., Bisby A., Beaudoin Y., Labossiere P. (1998) “Effects of Freeze-Thaw Action on the Bond of FRP Sheets to Concrete,” *Proceedings from the First International Conference on Durability of Fiber Reinforced Polymer (FRP) Composites for Construction*, 179-190.

Jones, F. R. (1999) “Durability of Reinforced Plastics in Liquid Environments,” Reinforced Plastics Durability, G. Pritchard, Ed., Woodhead Publishing Company, 70-110.

Kato Y., Yamaguchi T., Nishimura T., and Uomoto T. (1997) “Computational Model for Deterioration of Aramid Fiber by Ultraviolet Rays,” Non-metallic (FRP) Reinforcement for Concrete Structures,” *Proceedings of the 3rd International Symposium*, 2, 163-170.

Murphy, K., Zhang, S., and Karbhari, V. M. (1999) “Effects of concrete based alkaline solutions on short term response of composites,” *Proceedings of the44th Int. SAMPE Symposium and Exhibition*, Society for the Advancement of Material and Process Engineering, 2222-2230.

Porter M. L., Barnes B. A. (1998) "Accelerated Aging Degradation of Glass Fiber Composites," Fiber Composites in Infrastructure, *Proceedings of the Second International Conference on Fiber Composites in Infrastructure ICCI'98*, 2, 446-459.

Rahman A.H., Kingsley C., Richard J., and Crimi J. (1998) "Experimental Investigation of the Mechanism of Deterioration of FRP Reinforcement for Concrete," Fiber Composites in Infrastructure, *Proceedings of the Second International Conference on Fiber Composites in Infrastructure ICCI'98*, 2, 501-511.

Saadatmanesh H., and Tannous F. (1997) "Durability of FRP Rebars and Tendons," Non-Metallic (FRP) Reinforcement for Concrete Structures, *Proceedings of the Third International Symposium*, 2, 147-154.

Sasaki I., Nishizaki I., Sakamoto H., Katawaki K., and Kawamoto Y. (1997) "Durability Evaluation of FRP Cables by Exposure Tests," Non-metallic (FRP) Reinforcements for Concrete Structures, *Proceedings of the 3rd International Symposium*, 2, 131-137.

Shen, C. H., and Springer, G. S. (1976) "Moisture Absorption and Desorption in Composite Materials," *Journal of Composite Materials*, 10, 2-20, 1976.

Singh R. P., Nakamura T., and Kumar B. G., http://www.ic.sunysb.edu/stu/bgirishk/Research-QUV.htm, Department of Mechanical Engineering at SUNY, Stony Brook.

Tannous F. E., and Saadatmanesh H. (1998) "Durability and Long-Term Behavior of Carbon and Aramid FRP Tendons," Fiber Composites in Infrastructure, *Proceedings of the Second International Conference on Fiber Composites in Infrastructure ICCI'98*, 2, 524-538.

Uomoto T., and Nishimura T. (1997) "Development of New Alkali Resistance Hybrid A GFRP Rod," Non-metallic (FRP) reinforcement for Concrete Structures, *Proceedings of the 3rd International Symposium*, 2, 67-74.

Verghese N. E., Hayes M., Garcia K., Carrier C., Wood J., and Lesko J. J. (1998) "Effects of Temperature Sequencing During Hygrothermal Aging of Polymers and Polymer Matrix Composites: The Reverse Thermal Effect," Fiber Composites in Infrastructure, *Proceedings of the Second International Conference on Fiber Composites in Infrastructure ICCI'98*, 2, 720-739.

APPENDIX A. UNIAXIAL TENSION TEST DATA FOR DURABILITY OF GFRP SPECIMENS

A.1 Conditioning: Room temperature at 78.8°F and 35% Relative Humidity (Controlled Specimen)

Ultimate tensile strength: 15.07 ksi

Elastic modulus: 1074.4 ksi

Stress-strain curve:

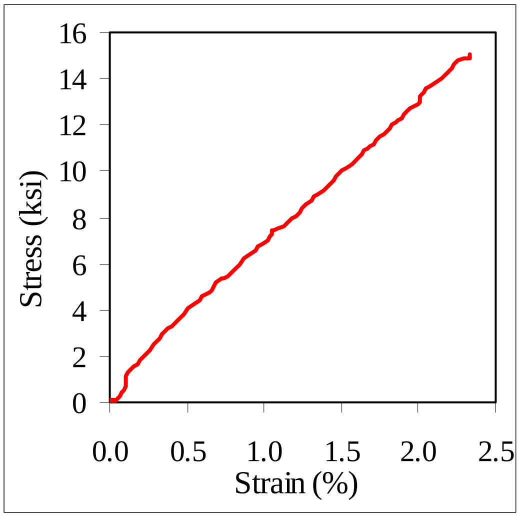

A.2 Conditioning: Freeze-Thaw Cycles

Ultimate tensile strength: 13.5 ksi

Elastic modulus: 878.10 ksi

Stress-strain curves:

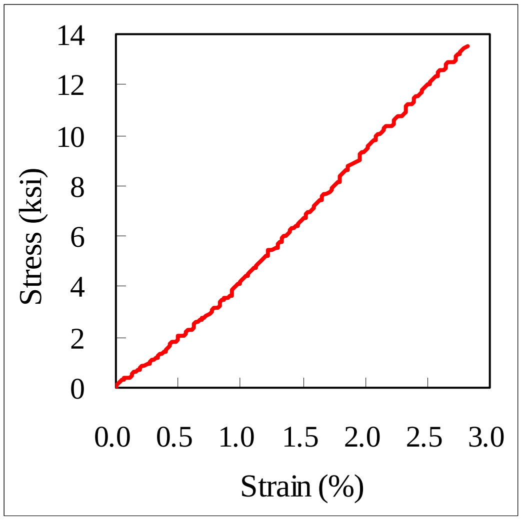

A.3 Conditioning: Wetting-Drying Cycles in Water

Ultimate tensile strength: 14.5 ksi

Elastic modulus: 785.47 ksi

Stress-strain curve:

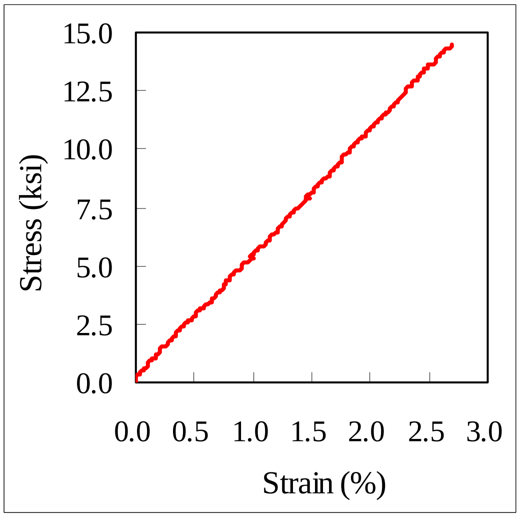

A.4 Conditioning: $Mg(Cl_2)$ 3% Ponding Test

Ultimate tensile strength: 13.16 ksi

Elastic modulus: 797.46 ksi

Stress-strain curve:

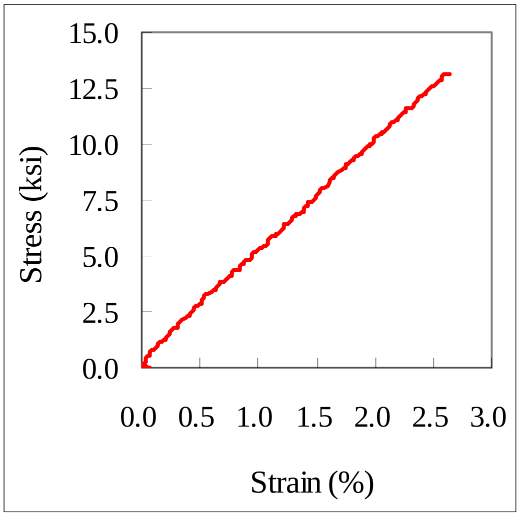

A.5 Conditioning: $Ca(Cl_2)$ 3% Ponding Test

Ultimate tensile strength: 13.20 ksi

Elastic modulus: 850.24 ksi

Stress-strain curve:

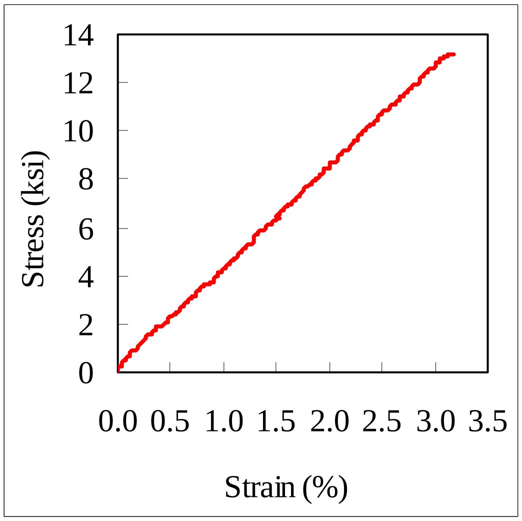

A.6 Conditioning: NaCl 3% Ponding Test

Ultimate tensile strength: 12.73 ksi

Elastic modulus: 768.75 ksi

Stress-strain curve:

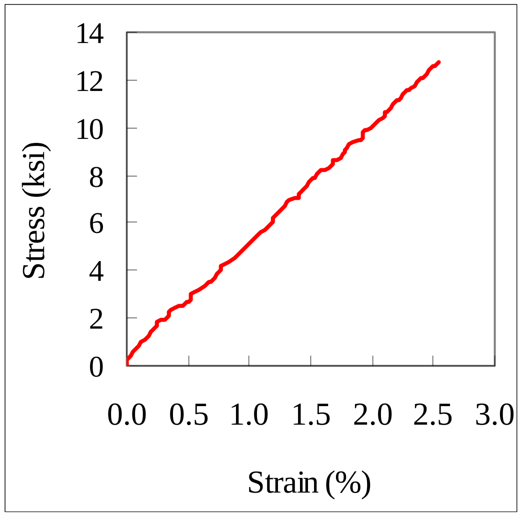

A.7 Conditioning: Mg(Cl$_2$) 3% Cyclic Test

Ultimate tensile strength: 13.44 ksi

Elastic modulus: 773.05 ksi

Stress-strain curve:

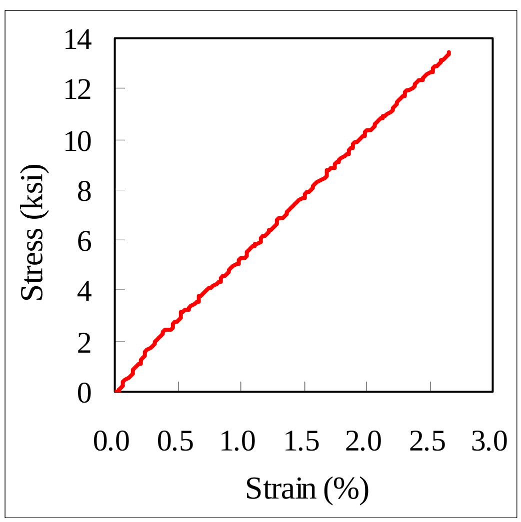

A.8 Conditioning: $Ca(Cl_2)$ 3% Cyclic Test

Ultimate tensile strength: 14.73 ksi

Elastic modulus: 726.45 ksi

Stress-strain curve:

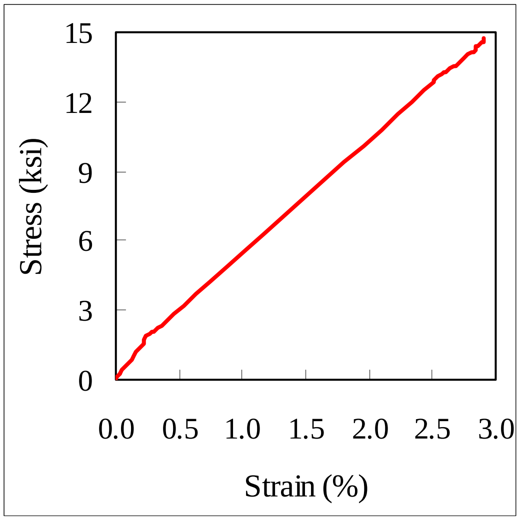

A.9 Conditioning: NaCl 3% Cyclic Test

Ultimate tensile strength: 11.50 ksi

Elastic modulus: 768.75 ksi

Stress-strain curve:

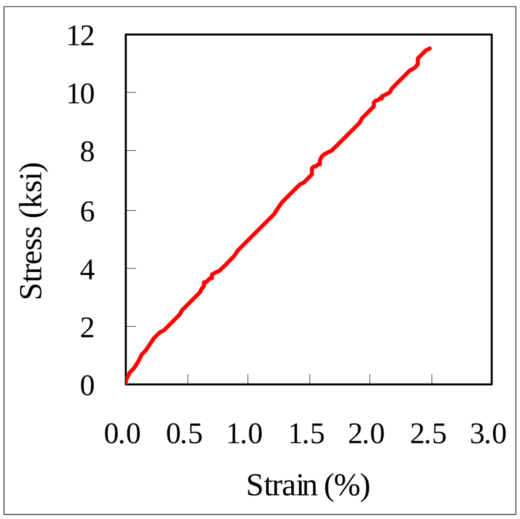

A.10 Conditioning: 1M NaOH Ponding Test

Ultimate tensile strength: 9.78 ksi

Elastic modulus: 773.87 ksi

Stress-strain curve:

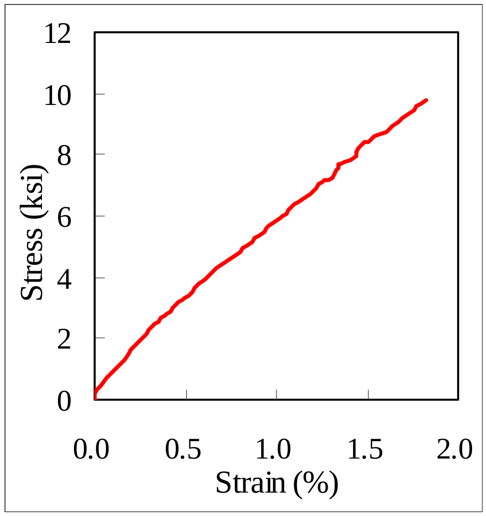

A.11 Conditioning: 1M HCl Ponding Test

Ultimate tensile strength: 14.13 ksi

Elastic modulus: 804.02 ksi

Stress-strain curve:

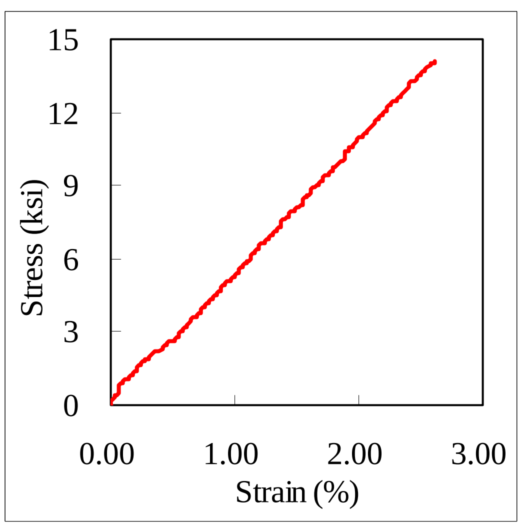

A.12 Conditioning: Ultraviolet Radiation Test

Ultimate tensile strength: 11.69 ksi

Elastic modulus: 763.92 ksi

Stress-strain curve:

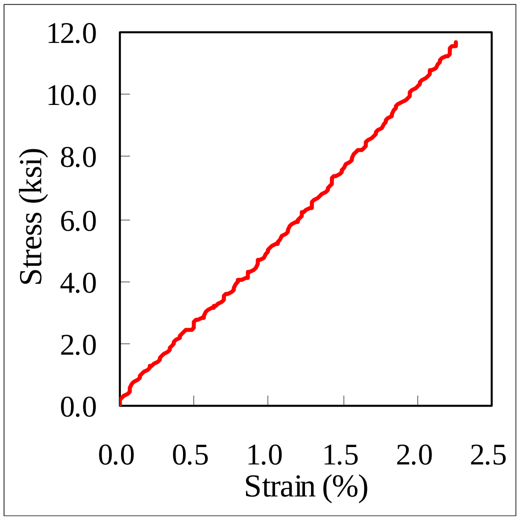

APPENDIX B. STRAIN HISTORY OF O'FALLON PARK BRIDGE DUE TO TEMPERATURE EFFECT

Date	Time	Temperature on the Panel 1 (°F)		Fiber Optic Sensor Locations									
		Top	Bottom	1	2	3	4	5	6	7	8	9	10
Sep 12 2003	9:30	71.42	54.68	10903	14454	14532	11928	13889	13669	13362	14791	14401	14166
	9:35			10928	14476	14551	11942	13905	13691	13378	14806	14421	14182
	9:40			10955	14497	14565	11957	13920	14132	13393	14817	14437	14199
	9:45			10982	14517	14584	11972	13936	14156	13405	14827	14456	14218
	9:50			11004	14540	14601	11986	13950	14184	13421	14839	14476	14236
	9:55			11027	14561	14618	12000	13966	14209	13435	14849	14494	14256
	10:00	80.06	55.40	11049	14584	14636	12015	13982	14226	13450	14861	14515	14276
	10:05			11075	14605	14654	12029	13998		13467	14874	14533	14293
	10:10			11093	14627	14670	12043	14013	13888	13477	14882	14557	14311
	10:15			11112	14650	14685	12058	14029	13914	13493	14894	14579	14330
	10:20			11129	14671	14702	12073	14044	13937	13509	14905	14599	14346
	10:25			11146	14691	14717	12090	14058	13953	13520	14922	14618	14361
	10:30	84.74	56.48	11165	14712	14734	12105	14074	13975	13535	14931	14635	14375
	10:35			11183	14733	14748	12122	14089	14007	13548	14943	14653	14389
	10:40			11203	14756	14765	12135	14103	14022	13561	14955	14675	14406
	10:45			11225	14777	14780	12144	14119	14047	13576	14970	14695	14422
	10:50			11246	14799	14797	12156	14136	14074	13590	14982	14712	14439
	10:55			11271	14822	14816	12170	14151	14100	13605	14992	14728	14456
	11:00	93.20	57.02	11295	14847	14829	12184	14166	14499	13620	15004	14748	14472
	11:05			11318	14864	14843	12200	14182		13634	15016	14769	14489
	11:10	93.92	57.74	11343	14880	14857	12217	14194		13647	15022	14783	14504
Feb 17 2004	10:00	27.10	31.80	8498	13940	14136	11520	13464	13058	12943	14427	13909	13744
	10:05	26.60	31.70	8499	13940	14134	11521	13465	13064	12945	14425	13910	13744
	10:10	26.40	32.70	8499	13942	14134	11521	13466	13068	12945	14427	13912	13745
	10:15	25.90	35.00	8500	13944	14133	11523	13466	13065	12943	14426	13911	13744
	10:20	25.70	34.70	8501	13943	14135	11523	13468	13063	12944	14431	13912	13745
	10:25	25.30	35.70	8503	13943	14134	11525	13470	13067	12946	14430	13912	13746
	10:30	25.00	35.90	8503	13942	14134	11525	13471	13073	12947	14433	13913	13746
	10:35	25.00	36.40	8504	13944	14133	11527	13472	13073	12951	14433	13914	13747
	10:40	24.80	36.80	8507	13944	14134	11528	13474	13074	12951	14430	13912	13748
	10:45	24.60	37.10	8508	13946	14135	11527	13473	13069	12952	14430	13915	13750
	10:50	24.40	37.80	8509	13947	14135	11529	13475	13071	12952	14434	13915	13748
	10:55	24.40	38.40	8511	13949	14134	11530	13476	13070	12955	14436	13915	13750
	11:00	24.40	37.70	8512	13948	14134	11531	13480	13082	12955	14437	13914	13751
	11:05	24.40	36.00	8512	13950	14133	11534	13481	13070	12955	14437	13914	13751
	11:10	24.40	35.10	8514	13951	14132	11533	13483	13081	12959	14439	13916	13754
	11:15	24.60	34.00	8515	13953	14134	11536	13484	13073	12961	14442	13914	13754
	11:20	24.60	34.40	8517	13954	14133	11536	13487	13073	12963	14441	13918	13755
	11:25	24.80	34.50	8517	13956	14133	11537	13488	13080	12967	14442	13918	13756
	11:30	24.80	34.50	8519	13958	14133	11539	13490	13079	12968	14441	13921	13755
	11:35	24.80	34.50	8520	13957	14134	11540	13489	13078	12971	14446	13922	13757
	11:40	24.80	34.40	8522	13957	14133	11540	13491	13075	12973	14449	13921	13759

	11:45	24.80	34.00	8524	13960	14135	11542	13491	13074	12974	14449	13925	13757
	11:50	25.00	33.80	8525	13960	14135	11544	13496	13084	12975	14450	13925	13761
	11:55	25.00	34.90	8526	13962	14132	11545	13496	13070	12980	14449	13928	13762
	12:00	25.20	36.40	8529	13963	14134	11545	13497	13070	12979	14450	13928	13762

Date	Time	Temperature on the Panel 1 (°F)		Fiber Optic Sensor Locations									
		Top	Bottom	11	12	13	14	15	16	17	18	19	20
Sep 12 2003	9:30	71.42	54.68	14308	14512	15402	12478	14154	14514	14814	14552	13146	14622
	9:35			14312	14515	15403	12482	14159	14530	14816	14561	13143	14627
	9:40			14315	14521	15410	12487	14167	14543	14819	14569	13153	14633
	9:45			14319	14525	15410	12493	14177	14557	14821	14576	13154	14641
	9:50			14322	14530	15413	12498	14184	14569	14825	14586	13161	14649
	9:55			14326	14537	15413	12502	14194	14583	14825	14595	13164	14655
	10:00	80.06	55.40	14330	14543	15421	12506	14200	14592	14828	14600	13174	14666
	10:05			14333	14546	15424	12512	14207	14609	14830	14612	13178	14675
	10:10			14336	14551	15430	12516	14215	14620	14834	14620	13179	14684
	10:15			14340	14558	15430	12521	14223	14632	14837	14631	13189	14691
	10:20			14342	14564	15436	12526	14232	14647	14840	14639	13197	14699
	10:25			14347	14569	15440	12531	14241	14662	14844	14646	13202	14708
	10:30	84.74	56.48	14348	14576	15443	12536	14249	14674	14845	14657	13202	14716
	10:35			14353	14582	15447	12543	14257	14689	14848	14664	13211	14726
	10:40			14356	14589	15454	12550	14266	14701	14851	14674	13211	14734
	10:45			14360	14597	15459	12557	14277	14717	14855	14681	13218	14745
	10:50			14364	14604	15463	12561	14285	14730	14858	14693	13224	14753
	10:55			14368	14615	15469	12570	14294	14742	14860	14701	13228	14762
	11:00	93.20	57.02	14370	14622	15478	12577	14305	14755	14862	14709	13239	14771
	11:05			14374	14632	15482	12583	14315	14768	14866	14716	13239	14780
	11:10	93.92	57.74	14378	14642	15488	12591	14323	14782	14869	14728	13250	14787
Feb 17 2004	10:00	27.10	31.80	13837	14159	15135	12127	13844	14132	14443	14139	12832	14262
	10:05	26.60	31.70	13839	14159	15135	12128	13844	14136	14443	14142	12832	14264
	10:10	26.40	32.70	13838	14158	15132	12127	13846	14134	14444	14141	13202	14263
	10:15	25.90	35.00	13839	14160	15135	12128	13845	14133	14443	14142	12833	14264
	10:20	25.70	34.70	13840	14159	15133	12128	13845	14137	14445	14143	12832	14263
	10:25	25.30	35.70	13838	14158	15133	12128	13845	14141	14443	14143	12837	14263
	10:30	25.00	35.90	13840	14158	15133	12129	13846	14140	14444	14145	12834	14261
	10:35	25.00	36.40	13840	14157	15136	12127	13847	14143	14444	14144	12833	14263
	10:40	24.80	36.80	13840	14158	15135	12128	13848	14143	14445	14146	12836	14262
	10:45	24.60	37.10	13840	14158	15135	12130	13850	14148	14446	14147	12835	14263
	10:50	24.40	37.80	13841	14160	15135	12132	13850	14146	14447	14148	12835	14263
	10:55	24.40	38.40	13842	14159	15134	12130	13850	14147	14447	14149	12832	14263
	11:00	24.40	37.70	13842	14160	15134	12133	13851	14149	14448	14149	12835	14264
	11:05	24.40	36.00	13843	14159	15137	12131	13852	14154	14447	14150	12839	14264
	11:10	24.40	35.10	13842	14162	15136	12132	13854	14155	14448	14153	12837	14264
	11:15	24.60	34.00	13842	14162	15135	12133	13856	14158	14448	14153	12837	14264

	11:20	24.60	34.40	13841	14162	15136	12136	13857	14159	14449	14155	12840	14265
	11:25	24.80	34.50	13844	14161	15139	12135	13858	14162	14450	14156	13206	14264
	11:30	24.80	34.50	13843	14163	15138	12136	13860	14165	14451	14155	12838	14266
	11:35	24.80	34.50	13845	14162	15136	12137	13860	14164	14452	14157	12841	14265
	11:40	24.80	34.40	13843	14163	15139	12138	13861	14167	14453	14157	12842	14267
	11:45	24.80	34.00	13845	14164	15138	12138	13862	14169	14454	14159	12839	14267
	11:50	25.00	33.80	13846	14162	15138	12139	13863	14170	14454	14160	12842	14267
	11:55	25.00	34.90	13846	14166	15138	12138	13864	14170	14456	14161	12841	14269
	12:00	25.20	36.40	13847	14164	15137	12138	13865	14174	14456	14161	12839	14268